

Extremal correlation coefficient for functional data

Mihyun Kim¹ and Piotr Kokoszka²

¹Department of Statistics, West Virginia University, Morgantown, WV, USA

²Department of Statistics, Colorado State University, Fort Collins, CO, USA

Address for correspondence: Mihyun Kim, Department of Statistics, West Virginia University, Morgantown, WV 26506, USA. Email: mihyun.kim@mail.wvu.edu

Abstract

We propose a coefficient that measures dependence in paired samples of functions. It has properties similar to the Pearson correlation, but differs in significant ways: 1) it is designed to measure dependence between curves, 2) it focuses only on extreme curves. The new coefficient is derived within the framework of regular variation in Banach spaces. A consistent estimator is proposed and justified by an asymptotic analysis and a simulation study. The usefulness of the new coefficient is illustrated on financial and climate functional data.

Keywords: correlation, extremes, functional data.

1 Introduction

Due to the growing impact of extreme events related, for example, to financial downturns or unusual weather, there has been increasing interest in developing statistical tools to study patterns of extreme curves. This is to a large extent due to the increasing availability of high resolution data; time series of asset prices can be constructed at practically any temporal resolution, and modern weather databases contain measurements at hourly or even higher frequencies. Such data can be interpreted as curves, e.g., one curve per day, and provide more complete information than a single number per day, like the total return or the maximum temperature. We propose a coefficient that quantifies the tendency of paired extreme curves to exhibit similar patterns simultaneously. Two examples of the type of questions that the tool deals with are the following: 1) During a stock market crisis, such as the market decline due to the COVID-19 pandemic, do returns of different sectors of the economy exhibit similar extreme daily trajectories? 2) How likely is location A to experience a similar daily pattern of temperature as location B (on the same day) during a heat wave? The coefficient we propose focuses not just on extreme total return or extreme maximum daily temperature, but also on the shapes of extreme curves.

There has been some research focusing on probabilistic and statistical methods for extreme curves. Extreme value theory in the space of continuous functions is studied in Chapters 9 and 10 of de Haan and Ferreira (2000). Principal component analysis of extreme curves has been studied by Kokoszka *et al.* (2019), Kokoszka and Kulik (2023), and Cl emen con *et al.* (2024). Extremal properties of scores of functional data were

studied by Kokoszka and Xiong (2018) and Kim and Kokoszka (2019, 2022). Additional, more closely related papers are introduced as we develop our approach. We propose a method for quantifying extremal dependence of paired functional samples, for which there are currently no appropriate tools.

We note that there has been considerable research aimed at quantifying extremal dependence for heavy-tailed random vectors. Ledford and Tawn (1996, 1997, 2003) introduced the *coefficient of tail dependence*, which was later generalized to the *extremogram* by Davis and Mikosch (2009). The *extremal dependence measure* based on the angular measure of a regularly varying random vector was introduced by Resnick (2004) and further investigated by Larsson and Resnick (2012). Janßen *et al.* (2023) recently introduced a unified approach for representing tail dependence using random exceedence sets. Those measures for extremes are designed for random vectors in a Euclidean space. Thus applying any such measures to functional data requires some sort of dimension reduction, e.g., principal component analysis, or data compression like converting daily temperature curves to daily average or maximum values. The reduced data are then analyzed using those tools for multivariate extremes, see, e.g., Meiguët (2010), Dombry and Ribatet (2015), and Kim and Kokoszka (2022). This approach is convenient, but it does not fully utilize all relevant information that functional data contain.

We develop a new measure, the *extremal correlation coefficient*, that captures the extremal dependence of paired functional samples utilizing the information in the sizes and shapes of the curves. The measure is constructed by computing an inner product of pairs of extreme curves. This approach is closely related to the concept of *cosine similarity* that is often used, for example, to quantify document similarity in text analysis. While the *cosine similarity* computes the inner product between two vectors to see whether they are pointing in the same direction using all available pairs, our measure calculates the inner product between paired extreme curves to see whether they look alike in extremes. Similar ideas have been applied in non-extreme contexts of functional data analysis. Dubin and Müller (2005) introduced a measure, called *dynamical correlation*, that computes the inner product of all pairs of standardized curves. The concept was further studied by Yeh *et al.* (2023) where an autocorrelation measure, termed *spherical autocorrelation*, for functional time series was proposed. These measures are however computed based on the total body of functional data, and so are not suitable for describing extremal dependence.

The coefficient we develop quantifies extremal dependence in pairs of heavy-tailed functional observations. It is conceptually appealing, as it shares desirable features with the classic correlation coefficient: 1) its values range from -1 to 1, 2) it measures the strength and direction of linear relationship between two extreme curves, 3) if the extremal behavior of two curves is independent, the coefficient is zero. Moreover, it can be used in practice with a relatively simple numerical implementation. We thus hope that such interpretable and tractable tool makes a useful contribution. No measures of extremal

dependence for pairs of curves are currently available.

Turning to mathematical challenges, the concept of vague convergence, see e.g., Chapters 2 and 6 of Resnick (2007), cannot be readily used. The vague convergence, which now provides a standard mathematical framework for extremes in Euclidean spaces, can be defined only on locally compact spaces. Since every locally compact Banach space has finite dimension, a different framework must be used for functional data in Hilbert spaces. We use the theory of regularly varying measures developed by Hult and Lindskog (2006) who introduced the notion of M_0 convergence, which works for regularly varying measures on complete separable metric spaces. The M_0 convergence is further studied by Meiguët (2010), where it is applied to regularly varying time series in a separable Banach space. Within this framework, to establish the consistency of the estimator we propose. To do so, we proceed through a number of M_0 convergence results that allow us to apply an abstract Bernstein-type inequality. A method of computing the extremal correlation coefficients analytically (in relatively simple cases) is also developed.

The remainder of the paper is organized as follows. In Section 2, we review regularly varying random elements in Banach spaces. In Section 3, we extend the concept of regular variation to bivariate random elements in a product Banach space. The extremal correlation coefficient is introduced in Section 4, where its asymptotic properties are also studied. Section 5 contains a simulation study, and Section 6 illustrates applications to intraday return curves and daily temperature curves.

Theoretical justification of our approach requires more detailed background and some technical derivations, which are placed in the online Supplementary Material. Preliminary results for the proof of Theorem 4.1 are presented in Section A, followed by its proof in Section B. In Section C, the proof of Lemma 5.1 is presented.

2 Regular variation in Banach spaces

This section presents background needed to understand the development in Sections 3 and 4. In Functional Data Analysis, observations are typically treated as elements of $L^2 := L^2(\mathcal{T})$, where the measure space \mathcal{T} is such that $L^2(\mathcal{T})$ is a *separable* Hilbert space, equipped with the usual inner product $\langle x, y \rangle = \int_{\mathcal{T}} x(t)y(t)dt$. The L^2 -norm is then $\|x\| = \langle x, x \rangle^{1/2} = \left(\int_{\mathcal{T}} x(t)^2 dt\right)^{1/2}$. An introduction to Functional Data Analysis is presented in Kokoszka and Reimherr (2017), while a detailed mathematical treatment is given in Hsing and Eubank (2015). While we refer to the elements of L^2 as curves, due to the examples we consider, the set \mathcal{T} can be a fairly abstract space (a metric Polish space), for example a spatial domain.

An extreme curve in L^2 is defined as a functional object whose size, measured by the L^2 -norm, is large. The norm can be large for various reasons as long as the area under the squared curve on \mathcal{T} is large. For example, curves that are far away from the sample

mean or that fluctuate a lot around the sample mean will be extreme according to this definition. Extreme functional observations are thus very different from extreme scalar or multivariate observations because there is a multitude of ways in which a curve can be extreme. We informally call functional data heavy-tailed if the probability that an extreme curve occurs is relatively large.

We now briefly review the M_0 convergence in a separable Banach space \mathbb{B} . In what follows, $\mathbf{0}$ is the zero element. Fix a norm $\|\cdot\|_{\mathbb{B}}$ and let $B_\varepsilon := \{z \in \mathbb{B} : \|z\|_{\mathbb{B}} < \varepsilon\}$ be the open ball of radius $\varepsilon > 0$ centered at the origin. A Borel measure μ defined on $\mathbb{B}_0 := \mathbb{B} \setminus \{\mathbf{0}\}$ is said to be *boundedly finite* if $\mu(A) < \infty$, for all Borel sets that are bounded away from $\mathbf{0}$, i.e., $A \cap B_\varepsilon = \emptyset$, for some $\varepsilon > 0$. Let $M_0(\mathbb{B})$ be the collection of all such measures on \mathbb{B}_0 . For $\mu_n, \mu \in M_0(\mathbb{B})$, the sequence of μ_n converges to μ in the M_0 topology ($\mu_n \xrightarrow{M_0} \mu$), if $\mu_n(A) \rightarrow \mu(A)$, for all bounded away from $\mathbf{0}$, μ -continuity Borel sets A , i.e., those with $\mu(\partial A) = 0$, where ∂A is the boundary of A . Equivalently, $\mu_n \xrightarrow{M_0} \mu$, if $\int_{\mathbb{B}} f(x) \mu_n(dx) \rightarrow \int_{\mathbb{B}} f(x) \mu(dx)$ for all $f \in \mathcal{C}_0(\mathbb{B})$, where $\mathcal{C}_0(\mathbb{B})$ is the class of bounded and continuous functions $f : \mathbb{B}_0 \rightarrow \mathbb{R}$ that vanish on a neighborhood of $\mathbf{0}$.

We now define regular variation for random elements in \mathbb{B} , see Theorem 3.1 of Hult and Lindskog (2006) and Chapter 2 of Meignat (2010). This concept formalizes the idea of heavy-tailed observations in infinite dimensional spaces.

DEFINITION 2.1 A random element X in \mathbb{B} is regularly varying with index $-\alpha$, $\alpha > 0$, if there exist a sequence $b(n) \rightarrow \infty$ and a measure μ in $M_0(\mathbb{B})$ such that

$$(2.1) \quad nP\left(\frac{X}{b(n)} \in \cdot\right) \xrightarrow{M_0} \mu, \quad n \rightarrow \infty,$$

where the exponent measure μ satisfies $\mu(tA) = t^{-\alpha}\mu(A)$ for Borel sets $A \subset \mathbb{B}_0$.

A possible choice for $b(n)$ is the quantile function, defined by $P(\|X\|_{\mathbb{B}} > b(n)) = n^{-1}$. Roughly speaking, the tail probability of X decays like a power function, $P(\|X\|_{\mathbb{B}} > t) \approx Ct^{-\alpha}$, as $t \rightarrow \infty$. The following lemma, see Hult and Lindskog (2006), states an equivalent definition of a regularly varying element in \mathbb{B} .

LEMMA 2.1 A random element X in \mathbb{B} is regularly varying with index $-\alpha$, $\alpha > 0$, if and only if there exist a sequence $b'(n) \rightarrow \infty$ and a probability measure Γ on $\mathbb{S} := \{x \in \mathbb{B} : \|x\|_{\mathbb{B}} = 1\}$ (called the angular measure) such that for any $y > 0$,

$$(2.2) \quad nP(\|X\|_{\mathbb{B}} > b'(n)y, X/\|X\|_{\mathbb{B}} \in \cdot) \xrightarrow{w} cy^{-\alpha}\Gamma, \quad n \rightarrow \infty,$$

for some $c > 0$.

If Definition 2.1 (or condition (2.2)) holds, we write $X \in RV(-\alpha, \Gamma)$. The polar representation (2.2) provides an intuitive interpretation of regular variation in \mathbb{B} . It

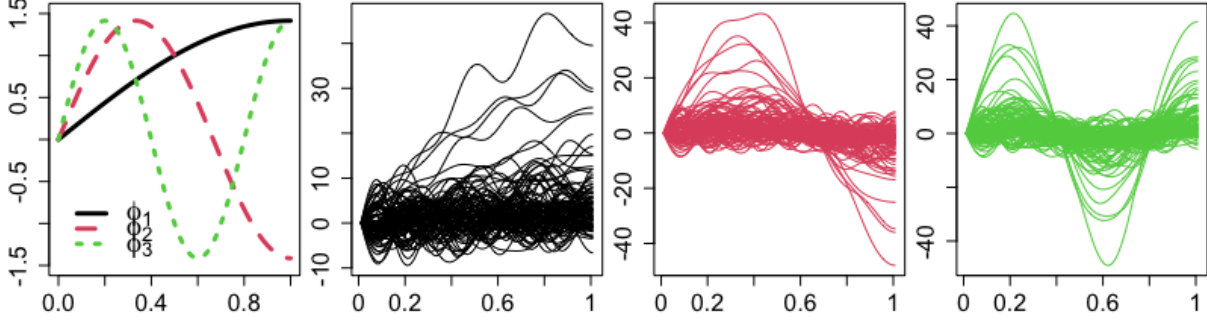


Figure 1: The first three orthonormal basis elements in $L^2[0, 1]$ defined in (2.3) (left-most); simulated data when Γ concentrates on ϕ_1 (second from the left); on ϕ_2 (third left); on ϕ_3 (fourth left).

characterizes regular variation of X in \mathbb{B} using two components, the tail index α and the angular probability measure Γ . The tail index α quantifies how heavy the tail distribution of $\|X\|_{\mathbb{B}}$ is, e.g., the probability of extreme curves occurring gets higher as α gets smaller. While the tail index α determines the frequency of occurrence of extreme curves, the angular measure Γ , defined on the unit sphere \mathbb{S} , fully characterizes the distribution of the shape of the scaled extreme curves, $X/\|X\|_{\mathbb{B}}$. To illustrate this, consider a set of orthonormal functions in $L^2([0, 1])$ of the form

$$(2.3) \quad \phi_j(t) = \sqrt{2} \sin \left(\left(j - \frac{1}{2} \right) \pi t \right), \quad j = 1, 2, \dots, \quad t \in [0, 1].$$

The first three functions are shown in the left-most plot of Figure 1. We consider a finite-dimensional subspace of $L^2([0, 1])$, spanned by the first 9 ϕ_j 's, for the purpose of simulations. The data generating process is $X(t) = \sum_{j=1}^9 Z_j \phi_j(t)$, where $\mathbf{Z} = [Z_1, \dots, Z_9]$ is a 9-dimensional random vector with independent components. Suppose that Z is a random variable following a Pareto distribution with tail index $\alpha = 3$ and N is a normal random variable with mean 0 and variance .5. We consider the following three cases for \mathbf{Z} :

1. $\mathbf{Z} = [Z, N, N, N, \dots, N]^T$; the angular measure Γ concentrates on ϕ_1 .
2. $\mathbf{Z} = [N, Z, N, N, \dots, N]^T$; the angular measure Γ concentrates on ϕ_2 .
3. $\mathbf{Z} = [N, N, Z, N, \dots, N]^T$; the angular measure Γ concentrates on ϕ_3 .

Figure 1 displays simulated data with sample size of 100 for each of the three cases. The plots of simulated data clearly show that the angular measure Γ represents the distribution of the shapes of extreme curves in that they are dominated by the shape of the functional axis ϕ_j on which Γ concentrates.

3 Bivariate regular variation in Banach spaces

In order to describe the extremal dependence of two regularly varying random elements X and Y in L^2 , we need to identify their *joint* probabilistic behavior. We again study it in the more general space \mathbb{B}^2 . We propose the following definition.

DEFINITION 3.1 A bivariate random element $[X, Y]^\top$ in \mathbb{B}^2 is said to be *jointly* regularly varying with index $-\alpha$, $\alpha > 0$, if there exist a sequence $b(n) \rightarrow \infty$ and a measure μ in $M_0(\mathbb{B}^2)$ such that

$$(3.1) \quad nP\left(\frac{(X, Y)}{b(n)} \in \cdot\right) \xrightarrow{M_0} \mu, \quad n \rightarrow \infty,$$

where the *joint* exponent measure μ satisfies $\mu(tA) = t^{-\alpha}\mu(A)$ for Borel sets $A \subset \mathbb{B}_0^2$.

We assume that one-dimensional marginal distributions of μ are non-degenerate, i.e., $\mu_X := \mu(\cdot \times \mathbb{B})$ and $\mu_Y := \mu(\mathbb{B} \times \cdot)$ are measures in $M_0(\mathbb{B})$ satisfying analogs of (2.1). Since X and Y are normalized by the same function $b(n)$, the marginal distributions are tail equivalent. A possible choice for $b(n)$ is the quantile function, defined by

$$P(\|(X, Y)\|_{\mathbb{B}^2} > b(n)) = n^{-1}.$$

With this choice, we have that

$$nP\left(\frac{(X, Y)}{b(n)} \in \mathcal{A}_1\right) = \frac{P((X, Y) \in b(n)\mathcal{A}_1)}{P(\|(X, Y)\|_{\mathbb{B}^2} > b(n))} = \frac{P((X, Y) \in \mathcal{A}_{b(n)})}{P((X, Y) \in \mathcal{A}_{b(n)})} = 1,$$

where \mathcal{A}_r is defined by

$$(3.2) \quad \mathcal{A}_r = \{(x, y) \in \mathbb{B}^2 : \|(X, Y)\|_{\mathbb{B}^2} \geq r\}, \quad r > 0.$$

Thus, it follows from the M_0 convergence in (3.1) and Lemma A.1 that

$$(3.3) \quad \mu(\mathcal{A}_1) = \mu\{(x, y) \in \mathbb{B}^2 : \|(X, Y)\|_{\mathbb{B}^2} > 1\} = 1,$$

which implies that μ is a probability measure on \mathcal{A}_1 . Throughout the paper, we set

$$\|(x, y)\|_{\mathbb{B}^2} := \|x\|_{\mathbb{B}} \vee \|y\|_{\mathbb{B}}.$$

This choice of norm works well with the *extremal correlation coefficient* defined in Section 4.

In order to derive the *joint* angular probability measure of X and Y , we consider the polar coordinate transformation $T : \mathbb{B}_0^2 \rightarrow ([0, \infty)^2 \setminus \{\mathbf{0}\}) \times \mathbb{S}^2$, defined by

$$(3.4) \quad T(x, y) = \left(\|x\|_{\mathbb{B}}, \|y\|_{\mathbb{B}}, \frac{x}{\|x\|_{\mathbb{B}}}, \frac{y}{\|y\|_{\mathbb{B}}}\right) =: (r_X, r_Y, \theta_X, \theta_Y), \quad (x, y) \in \mathbb{B}_0^2.$$

Using T , we obtain an equivalent formulation for a regularly varying random element in \mathbb{B}^2 .

PROPOSITION 3.1 *A bivariate random element $[X, Y]^\top$ in \mathbb{B}^2 is regularly varying with index $-\alpha$, $\alpha > 0$, if and only if there exists an exponent measure ν in $M_0([0, \infty)^2 \setminus \{\mathbf{0}\})$ and an angular probability measure Γ in $M_0(\mathbb{S}^2)$ such that*

$$(3.5) \quad nP \left(\frac{(\|X\|_{\mathbb{B}}, \|Y\|_{\mathbb{B}})}{b(n)} \in \cdot, (X/\|X\|_{\mathbb{B}}, Y/\|Y\|_{\mathbb{B}}) \in \cdot \right) \xrightarrow{M_0} \nu \times \Gamma, \quad n \rightarrow \infty,$$

where $b(n)$ is the increasing sequence in (3.1). (We note that μ in (3.1) is a measure on \mathbb{B}_0^2 , while ν in (3.5) is a measure on $[0, \infty)^2 \setminus \{\mathbf{0}\}$.)

PROOF: We only show that (3.1) implies (3.5) since showing the converse is similar. Take any $f \in \mathcal{C}_0([0, \infty)^2 \times \mathbb{S}^2)$. It then follows from the change of variables that

$$\begin{aligned} & \int_{[0, \infty)^2} \int_{\mathbb{S}^2} f(r_X, r_Y, \theta_X, \theta_Y) nP \left(\frac{(\|X\|_{\mathbb{B}}, \|Y\|_{\mathbb{B}})}{b(n)} \in (dr_X, dr_Y), \left(\frac{X}{\|X\|_{\mathbb{B}}}, \frac{Y}{\|Y\|_{\mathbb{B}}} \right) \in (d\theta_X, d\theta_Y) \right) \\ &= \int_{\mathbb{B}^2} f(T(x, y)) nP \left(\frac{X}{b(n)} \in dx, \frac{Y}{b(n)} \in dy \right). \end{aligned}$$

Since $f \in \mathcal{C}_0([0, \infty)^2 \times \mathbb{S}^2)$, there exists a set A , bounded away from $\mathbf{0}$ in $[0, \infty)^2 \times \mathbb{S}^2$, such that $f(T(x, y)) = 0$ if $T(x, y) \notin A$. Then we have that $f(T(x, y)) = 0$ if $(x, y) \notin T^{-1}(A)$. Since $T^{-1}(A)$ is bounded away from $\mathbf{0}$ in \mathbb{B}^2 , we have that $f \circ T \in \mathcal{C}_0(\mathbb{B}^2)$. Then by the M_0 convergence in Definition 3.1, we have that

$$\begin{aligned} & \int_{\mathbb{B}^2} (f \circ T)(x, y) nP \left(\frac{X}{b(n)} \in dx, \frac{Y}{b(n)} \in dy \right) \\ & \rightarrow \int_{\mathbb{B}^2} (f \circ T)(x, y) \mu(dx, dy) = \int_{T(\mathbb{B}^2)} f(r_X, r_Y, \theta_X, \theta_Y) \mu \circ T^{-1}(dr_X, dr_Y, d\theta_X, d\theta_Y). \end{aligned}$$

To investigate the form of $\mu \circ T^{-1}$, take any $t > 0$ and Borel set $S \subset \mathbb{S}^2$. It then follows from the homogeneity property of μ that

$$\begin{aligned} & \mu \circ T^{-1}([0, \infty)^2 \setminus [0, t]^2 \times S) \\ &= \mu \{ (x, y) \in \mathbb{B}_0^2 : \|x\|_{\mathbb{B}} \vee \|y\|_{\mathbb{B}} > t, (x/\|x\|_{\mathbb{B}}, y/\|y\|_{\mathbb{B}}) \in S \} \\ &= \mu \{ (x, y) \in \mathbb{B}_0^2 : \|x\|_{\mathbb{B}} \vee \|y\|_{\mathbb{B}} > t \} \times \\ & \quad \frac{t^{-\alpha} \mu \{ (x, y) \in \mathbb{B}_0^2 : \|x\|_{\mathbb{B}} \vee \|y\|_{\mathbb{B}} > 1, (x/\|x\|_{\mathbb{B}}, y/\|y\|_{\mathbb{B}}) \in S \}}{t^{-\alpha} \mu \{ (x, y) \in \mathbb{B}_0^2 : \|x\|_{\mathbb{B}} \vee \|y\|_{\mathbb{B}} > 1 \}}. \end{aligned}$$

It then follows from (3.3) that

$$\mu \circ T^{-1}([0, \infty)^2 \setminus [0, t]^2 \times S) = \nu([0, \infty)^2 \setminus [0, t]^2) \Gamma(S),$$

where

$$\begin{aligned} \nu(A) &:= \mu \{ (x, y) \in \mathbb{B}_0^2 : (\|x\|_{\mathbb{B}}, \|y\|_{\mathbb{B}}) \in A \}, \quad A \subset [0, \infty)^2 \setminus \{\mathbf{0}\}; \\ \Gamma(S) &:= \mu \{ (x, y) \in \mathbb{B}_0^2 : \|x\|_{\mathbb{B}} \vee \|y\|_{\mathbb{B}} > 1, (x/\|x\|_{\mathbb{B}}, y/\|y\|_{\mathbb{B}}) \in S \}, \quad S \subset \mathbb{S}^2. \end{aligned}$$

Thus, $\mu \circ T^{-1}$ has the product form such that on $([0, \infty)^2 \setminus \{\mathbf{0}\}) \times \mathbb{S}^2$

$$(3.6) \quad \mu \circ T^{-1} = \nu \times \Gamma,$$

which completes the proof. ■

Convergence (3.5) can be understood as a polar representation of the bivariate regular variation of $[X, Y]^\top$ in \mathbb{B}^2 . The difference between ν in (3.5) and μ in (3.1) is that μ describes the *joint* behavior of extreme curves X and Y in \mathbb{B}_0^2 , but ν describes extremal dependence between the sizes $\|X\|_{\mathbb{B}}$ and $\|Y\|_{\mathbb{B}}$ in $[0, \infty)^2 \setminus \mathbf{0}$. The *joint* behavior of X and Y in extremes is thus characterized by two measures, ν on $[0, \infty)^2 \setminus \{\mathbf{0}\}$ and Γ on \mathbb{S}^2 . The measure ν describes the joint behavior of $\|X\|_{\mathbb{B}}$ and $\|Y\|_{\mathbb{B}}$ in extremes. If ν has its mass only on the axes, then $\|X\|_{\mathbb{B}}$ and $\|Y\|_{\mathbb{B}}$ are asymptotically independent, i.e., if one curve shows an extreme behavior, there is negligible probability of the other curve also showing an extreme behavior. If ν has mass only on the line $\{t(1, 1), t > 0\}$, then $\|X\|_{\mathbb{B}}$ and $\|Y\|_{\mathbb{B}}$ show asymptotic full dependence, i.e., extreme curves occur simultaneously in X and Y .

We remark that the measure ν on $[0, \infty)^2 \setminus \mathbf{0}$ is homogeneous because for any $A \subset [0, \infty)^2 \setminus \{\mathbf{0}\}$ and $t > 0$,

$$\begin{aligned} \nu(tA) &= \mu \{(x, y) \in \mathbb{B}_0^2 : (\|x\|_{\mathbb{B}}, \|y\|_{\mathbb{B}}) \in tA\} \\ &= \mu \{t(x', y') \in \mathbb{B}_0^2 : (\|x'\|_{\mathbb{B}}, \|y'\|_{\mathbb{B}}) \in A\} \\ &= t^{-\alpha} \mu \{(x', y') \in \mathbb{B}_0^2 : (\|x'\|_{\mathbb{B}}, \|y'\|_{\mathbb{B}}) \in A\} \\ &= t^{-\alpha} \nu(A). \end{aligned}$$

The *joint* angular probability measure Γ characterizes how the shapes of scaled X and Y are related in extremes. If the extreme curves are exactly proportional, i.e., $X = \lambda Y$, $\lambda \neq 0$, the scaled curves share the same extreme functional elements. This means that Γ concentrates on the “line” $\{(\phi_j, \phi_j), j \in \mathcal{J} \subset \mathbb{N}\} \subset \mathbb{S}^2$, where $\{\phi_j, j \geq 1\}$ is a set of orthonormal elements in \mathbb{S} . If the shapes of two curves do not match in extremes, then Γ concentrates on $\{(\phi_j, \phi_k)\} \subset \mathbb{S}^2$, where $j \in \mathcal{J} \subset \mathbb{N}$, $k \in \mathcal{K} \subset \mathbb{N}$, $\mathcal{J} \cap \mathcal{K} = \emptyset$. This situation corresponds to vanishing extremal covariance defined in Section 4.

The *marginal* extreme behavior of X can be obtained by integrating all possible values of Y in (3.1), or $\|Y\|_{\mathbb{B}}, Y/\|Y\|_{\mathbb{B}}$ in (3.5). Then X has its *marginal* measure μ_X , and equivalently $X \in RV(-\alpha, \Gamma_X)$, where Γ_X is the *marginal* angular measure of X . Similarly, Y has its *marginal* μ_Y , and equivalently $Y \in RV(-\alpha, \Gamma_Y)$, where Γ_Y is the *marginal* angular measure of Y .

Table 1: The range of σ_{XY} , *extremal covariance* between X and Y , depending on the extremal dependence between $\|X\|$ and $\|Y\|$ and the level of similarity between $X/\|X\|$ and $Y/\|Y\|$ in extremes.

$\ X\ $ and $\ Y\ $ Asymptotic Independence	$\ X\ $ and $\ Y\ $ Asymptotic Dependence
$\sigma_{XY} = 0$	$X/\ X\ $ and $Y/\ Y\ $ look similar $\sigma_{XY} > 0$
	look orthogonal $\sigma_{XY} \approx 0$
	look opposite $\sigma_{XY} < 0$

4 Extremal correlation coefficient for functional data

In this section, we introduce the *extremal correlation coefficient* for functional data. It focuses on the extreme part of the *joint* distribution of regularly varying random elements X and Y in L^2 . It measures the tendency of paired curves to exhibit similar extreme patterns by computing a suitable inner product between X and Y conditional on large $[X, Y]^\top$.

Given a regularly varying bivariate random element $[X, Y]^\top$ in $L^2 \times L^2$ with *joint* exponent measure μ , we define the *extremal covariance* between X and Y by

$$(4.1) \quad \sigma_{XY} = \int_{\|x\| \vee \|y\| > 1} \langle x, y \rangle \mu(dx, dy).$$

Recall that by (3.3), $\mu I_{\{\|x\| \vee \|y\| > 1\}}$ is a probability measure. The *extremal covariance* is thus an extreme analog of the classic covariance in that σ_{XY} measures how much two random curves vary together in extremes. To see this more closely, we recall the transformation T defined in (3.4) and the relation $\mu \circ T^{-1} = \nu \times \Gamma$ in (3.6). It then follows from the change of variables that

$$(4.2) \quad \sigma_{XY} = \int_{r_X \vee r_Y > 1} r_X r_Y \nu(dr_X, dr_Y) \int_{\mathbb{S}^2} \langle \theta_X, \theta_Y \rangle \Gamma(d\theta_X, d\theta_Y).$$

The *extremal covariance* of X and Y can be thus factorized into the extremal dependence between $\|X\|$ and $\|Y\|$ and the level of similarity of the shapes between $X/\|X\|$ and $Y/\|Y\|$. If $\|X\|$ and $\|Y\|$ are asymptotically independent, i.e., extreme curves do not occur simultaneously, then ν concentrates on the coordinate axes. This implies that $\int_{r_X \vee r_Y > 1} r_X r_Y \nu(dr_X, dr_Y) = 0$, so $\sigma_{XY} = 0$ regardless of how X and Y look like in extremes. If $\|X\|$ and $\|Y\|$ are asymptotically dependent, i.e., extreme norms tend to occur simultaneously, then $\int_{r_X \vee r_Y > 1} r_X r_Y \nu(dr_X, dr_Y) > 0$ and so there are three possible ranges for σ_{XY} depending on the relative shape of extreme $X/\|X\|$ and $Y/\|Y\|$: 1) $\sigma_{XY} > 0$

if the shapes look similar, 2) $\sigma_{XY} \approx 0$ if the shapes do not match, i.e., the curves are orthogonal, or 3) $\sigma_{XY} < 0$ if they look opposite. These properties are summarized in Table 1.

We further define the *extremal correlation coefficient* by

$$(4.3) \quad \rho_{XY} = \frac{\sigma_{XY}}{\sigma_X \sigma_Y},$$

where

$$\sigma_X = \left\{ \int_{\|x\| \vee \|y\| > 1} \|x\|^2 \mu(dx, dy) \right\}^{1/2}, \quad \sigma_Y = \left\{ \int_{\|x\| \vee \|y\| > 1} \|y\|^2 \mu(dx, dy) \right\}^{1/2}.$$

The coefficient ρ_{XY} has properties analogous to the classic correlation coefficient: 1) $-1 \leq \rho_{XY} \leq 1$, 2) ρ_{XY} measures the strength and direction of linear relationships between X and Y in extremes, 3) If X and Y are independent, then $\rho_{XY} = 0$ since independence implies asymptotic independence between $\|X\|$ and $\|Y\|$.

To motivate our estimation approach, we first show that σ_{XY} is a limit of the expected inner product of X and Y conditional on large values of $[X, Y]^\top$.

PROPOSITION 4.1 *Let $[X, Y]^\top$ be a regularly varying random element in $L^2 \times L^2$. Then,*

$$\sigma_{XY} = \lim_{n \rightarrow \infty} E \left[\left\langle \frac{X}{b(n)}, \frac{Y}{b(n)} \right\rangle \middle| \|X\| \vee \|Y\| > b(n) \right].$$

PROOF: Considering $f : L^2 \times L^2 \rightarrow \mathbb{R}$ defined by $(x, y) \rightarrow \langle x, y \rangle I_{\|x\| \vee \|y\| > 1}$, we have that

$$\begin{aligned} & E \left[\langle b(n)^{-1} X, b(n)^{-1} Y \rangle \middle| \|X\| \vee \|Y\| > b(n) \right] \\ &= \frac{1}{P(\|X\| \vee \|Y\| > b(n))} E \left[\langle b(n)^{-1} X, b(n)^{-1} Y \rangle I_{\|X\| \vee \|Y\| > b(n)} \right] \\ &= \int_{L^2 \times L^2} f(x, y) \frac{P(b(n)^{-1} X \in dx, b(n)^{-1} Y \in dy)}{P(\|X\| \vee \|Y\| > b(n))}. \end{aligned}$$

Note that f is bounded and vanishes on a neighborhood of $\mathbf{0}$ in $L^2 \times L^2$. Also, the discontinuity set of f is the boundary of $\mathcal{A}_1 = \{(x, y) \in L^2 \times L^2 : \|x\| \vee \|y\| \geq 1\}$, and it follows from Lemma A.1 that $\mu(\partial \mathcal{A}_1) = 0$. Therefore, by (3.1) and Lemma A.1 of Meiguët (2010), we get the claim. ■

Based on Proposition 4.1, we propose an estimator for σ_{XY} defined by

$$(4.4) \quad \hat{\sigma}_{n,k} = \frac{1}{k} \sum_{i=1}^n \left\langle \frac{X_i}{R_{(k)}}, \frac{Y_i}{R_{(k)}} \right\rangle I_{R_i \geq R_{(k)}},$$

where $[X_i, Y_i]^\top, 1 \leq i \leq n$, are i.i.d. copies of $[X, Y]^\top$, $R_i := \|X_i\| \vee \|Y_i\|$ and $R_{(k)}$ is the k th largest order statistic with the convention $R_{(1)} = \max\{R_1, \dots, R_n\}$. An estimator for ρ_{XY} is then defined by

$$(4.5) \quad \hat{\rho}_{n,k} = \frac{\sum_{i=1}^n \langle X_i, Y_i \rangle}{\sqrt{\sum_{i=1}^n \|X_i\|^2} \sqrt{\sum_{i=1}^n \|Y_i\|^2}} I_{R_i \geq R_{(k)}}.$$

These estimators take only the k largest pairs of $[X_i, Y_i]^\top, 1 \leq i \leq n$, as inputs. This approach falls into so-called peaks-over-threshold framework in that it relies only on k largest observations whose magnitude exceeds a certain threshold. Asymptotic properties in this framework are typically derived as k goes to infinity with n , in such a way that $k/n \rightarrow 0$. We assume throughout the paper that this condition holds.

We will work under the following assumption.

ASSUMPTION 4.1 The bivariate random element $[X, Y]^\top$ in $L^2 \times L^2$ has mean zero and is regularly varying with index $-\alpha$, $\alpha > 2$. The observations $[X_1, Y_1]^\top, [X_2, Y_2]^\top, \dots$ are independent copies of $[X, Y]^\top$.

We state in the following theorem that the estimator $\hat{\sigma}_{n,k}$ is consistent for the *extremal covariance*. All proofs of the theoretical results introduced in this section are presented in Sections A and B of the Appendix, as they require a number of preliminary results and technical arguments.

THEOREM 4.1 *Under Assumption 4.1,*

$$\hat{\sigma}_{n,k} \xrightarrow{P} \sigma_{XY},$$

where $\hat{\sigma}_{n,k}$ and σ_{XY} are defined in (4.4) and (4.1), respectively.

From Theorem 4.1, the consistency of $\hat{\rho}_{n,k}$ for ρ_{XY} follows from Slutsky's theorem.

COROLLARY 4.1 *Under Assumption 4.1,*

$$\hat{\rho}_{n,k} \xrightarrow{P} \rho_{XY},$$

where $\hat{\rho}_{n,k}$ and ρ_{XY} are defined in (4.5) and (4.3), respectively.

We end this section with a discussion on the condition $\alpha > 2$ in Assumption 4.1. The condition is needed because the definition of extremal correlation coefficient presumes the existence of the second moment of the underlying processes. It can be lifted for the following alternative measure

$$(4.6) \quad \gamma_{XY} := \int_{\mathbb{S}^2} \langle \theta_X, \theta_Y \rangle \Gamma(d\theta_X, d\theta_Y),$$

which is the angular density factor in (4.2). This measure itself could be considered a measure for extremal correlation since $-1 \leq \gamma_{XY} \leq 1$. Just as Proposition 4.1, it can be shown that

$$\gamma_{XY} = \lim_{n \rightarrow \infty} E \left[\left\langle \frac{X}{\|X\|}, \frac{Y}{\|Y\|} \right\rangle \left| \|X\| \vee \|Y\| > b(n) \right. \right].$$

From this relation, an estimator for γ_{XY} can be defined by

$$\hat{\gamma}_{n,k} = \frac{1}{k} \sum_{i=1}^N \left\langle \frac{X_i}{\|X_i\|}, \frac{Y_i}{\|Y_i\|} \right\rangle I_{R_i \geq R_{(k)}},$$

and its consistency can be proven in almost the same manner as the proof of Corollary 4.2 of Cl  men  on *et al.* (2024), where $\alpha > 0$ is assumed.

Although the assumption $\alpha > 2$ could be relaxed by employing γ_{XY} as an extremal correlation measure, it should be noted that γ_{XY} does not account for whether extreme curves X and Y occur simultaneously, as ρ_{XY} in (4.3) does. To see this, suppose that $X = Z_1\phi$ and $Y = Z_2\phi$, where Z_1, Z_2 are independent random variables satisfying $P(Z_1 > z) = z^{-\alpha}$, $z > 0$, and ϕ is any unit norm element of L^2 . Then, $\gamma_{XY} = 1$, but $\rho_{XY} = 0$. One can argue that the measure $\rho_{XY} = 0$ is more appropriate because the extremes of X and Y occur independently, and the objective of our coefficient is to measure similarity of shapes in paired extreme curves. The identity $\rho_{XY} = 0$ holds because the measure ν in (4.2) concentrates on the coordinate axes, so

$$\sigma_{XY} = \int_{r_X \vee r_Y > 1} r_X r_Y \nu(dr_X, dr_Y) \int_{S^2} \langle \theta_X, \theta_Y \rangle \Gamma(d\theta_X, d\theta_Y) = 0 \times 1 = 0,$$

and the condition $\alpha > 2$ is needed for the first integral to exist.

5 A simulation study

We perform a simulation study to demonstrate that the proposed estimator, $\hat{\rho}_{n,k}$, consistently estimates the extremal correlation. We generate functional observations in such a way that the theoretical value of ρ_{XY} can be computed analytically, so that we can see how close $\hat{\rho}_{n,k}$ is to the true value.

The design of our study is as follows. Suppose that Z_1, Z_2 are i.i.d. random variables in \mathbb{R} satisfying $P(|Z_1| > z) = z^{-\alpha}$ with equal chance of Z_1 being either negative or positive. Also, let N_1, N_2, N_3 be i.i.d. normal random variables in \mathbb{R} with mean 0 and variance 1. Consider $\{\phi_j, j \geq 1\}$ defined by (2.3) and recall that it is an orthonormal basis in $L^2([0, 1])$. These functions are simulated on a grid of 100 equally-spaced points on the unit interval $[0, 1]$. We consider the following data generating processes, for $-1 \leq \rho \leq 1$,

$$(5.1) \quad \begin{aligned} X(t) &= Z_1\phi_1(t) + N_1\phi_2(t) + N_2\phi_3(t); \\ Y(t) &= \rho Z_1\phi_1(t) + (1 - \rho^2)^{1/2} Z_2\phi_2(t) + N_3\phi_3(t). \end{aligned}$$

Table 2: Empirical biases (standard errors) of $\hat{\rho}_{n,k}$ in (4.5) when $\alpha = 2.1$. The number of upper order statistics is $k = 2\lfloor n^{1/2} \rfloor$.

ρ_{XY}	$N = 100$	$N = 500$	ρ_{XY}	$N = 100$	$N = 500$
0	0.000 (0.051)	0.000 (0.023)			
0.1	0.005 (0.086)	0.015 (0.096)	-0.1	-0.008 (0.097)	-0.009 (0.070)
0.2	0.012 (0.138)	0.014 (0.107)	-0.2	-0.009 (0.133)	-0.016 (0.116)
0.3	-0.012 (0.159)	0.012 (0.137)	-0.3	0.002 (0.166)	-0.013 (0.142)
0.4	-0.021 (0.176)	0.007 (0.149)	-0.4	0.010 (0.180)	-0.011 (0.156)
0.5	-0.041 (0.178)	0.002 (0.164)	-0.5	0.030 (0.179)	0.008 (0.161)
0.6	-0.066 (0.180)	-0.011 (0.168)	-0.6	0.056 (0.180)	0.012 (0.162)
0.7	-0.071 (0.179)	-0.029 (0.153)	-0.7	0.076 (0.174)	0.032 (0.160)
0.8	-0.093 (0.155)	-0.040 (0.142)	-0.8	0.097 (0.158)	0.032 (0.138)
0.9	-0.112 (0.127)	-0.043 (0.108)	-0.9	0.111 (0.127)	0.041 (0.102)
1.0	-0.116 (0.066)	-0.040 (0.021)	-1.0	0.118 (0.069)	0.041 (0.021)

This generates extreme curves dominated by the shape of the functional axis ϕ_1 for X and by either ϕ_1 or ϕ_2 for Y . The following lemma gives an analytic formula for ρ_{XY} . Its proof is provided in Section C of the Appendix.

LEMMA 5.1 *Let $\mathbf{Z} = [Z_1, Z_2]^\top$ be a random vector in \mathbb{R}^2 consisting of iid components Z_j whose magnitude is regularly varying with tail index $\alpha > 2$, i.e., for some $c_+, c_- \geq 0$,*

$$P(Z_1 > z) \sim c_+ z^{-\alpha}, \quad P(Z_1 < -z) \sim c_- z^{-\alpha},$$

where $f(z) \sim g(z)$ if and only if $\lim_{z \rightarrow \infty} f(z)/g(z) = 1$. Also, let $\{\phi_j, j \geq 1\}$ be a set of orthonormal elements in \mathbb{S} . Then, for X and Y in (5.1),

$$\rho_{XY} = \frac{\rho}{\{\rho^2 + (1 - \rho^2)^{\alpha/2}\}^{1/2}}.$$

We consider $\rho_{XY} \in \{0, \pm 0.1, \pm 0.2, \dots, \pm 0.9, \pm 1\}$ and $\alpha \in \{2.1, 3, 4, 5\}$, from which values of ρ can be obtained by Lemma 5.1. For each ρ , we generate $[X_i, Y_i]^\top, 1 \leq i \leq N$, that are i.i.d. copies of $[X, Y]^\top$, with sample sizes $N \in \{100, 500\}$. In each case, 1000 replications are generated.

In order to compute $\hat{\rho}_{n,k}$ in (4.5), we must select k largest pairs of curves. We first consider $k = 2\lfloor N^{1/2} \rfloor$, where $\lfloor x \rfloor$ is the integer part of x , to demonstrate the performance of the estimator with a deterministic form of k . Additionally, we provide a method for determining the optimal value of k as a guiding tool in practical applications.

Our approach to identifying the optimal value of k is motivated by the theoretical property of the size of pairs, $R_i = \|X_i\| \vee \|Y_i\|$. By Lemma A.2 (i), if (X, Y) are regularly

Table 3: Empirical biases (standard errors) of $\hat{\rho}_{n,k}$ when $\alpha = 2.1$. The KS method is used to choose optimal k s. On average, it selects $k = 8$ ($N = 100$) and $k = 25 \sim 32$ ($N = 500$).

ρ_{XY}	$N = 100$	$N = 500$	ρ_{XY}	$N = 100$	$N = 500$
0	-0.001 (0.083)	0.000 (0.041)			
0.1	0.026 (0.139)	0.032 (0.127)	-0.1	-0.033 (0.153)	-0.026 (0.117)
0.2	0.042 (0.204)	0.033 (0.156)	-0.2	-0.043 (0.198)	-0.040 (0.179)
0.3	0.022 (0.225)	0.035 (0.190)	-0.3	-0.033 (0.228)	-0.032 (0.195)
0.4	0.013 (0.229)	0.023 (0.193)	-0.4	-0.023 (0.234)	-0.028 (0.204)
0.5	-0.006 (0.232)	0.019 (0.204)	-0.5	-0.006 (0.231)	-0.002 (0.215)
0.6	-0.032 (0.235)	0.006 (0.211)	-0.6	0.021 (0.233)	-0.002 (0.207)
0.7	-0.034 (0.221)	-0.019 (0.188)	-0.7	0.039 (0.217)	0.025 (0.198)
0.8	-0.049 (0.195)	-0.033 (0.173)	-0.8	0.054 (0.192)	0.024 (0.170)
0.9	-0.067 (0.153)	-0.032 (0.122)	-0.9	0.066 (0.146)	0.034 (0.124)
1.0	-0.064 (0.056)	-0.029 (0.026)	-1.0	0.065 (0.059)	0.030 (0.027)

varying in $L^2 \times L^2$ with tail index α , then $R = \|X\| \vee \|Y\|$ is also regularly varying in \mathbb{R}_+ with the same tail index α . Therefore, we choose k that results in successful tail estimation for R in finite samples. In the literature on tail estimation, various methods for selecting upper-order statistics have been introduced, e.g., Hall and Welsh (1985), Hall (1990), Drees and Kaufmann (1998), and Danielsson *et al.* (2001), just to name a few. We adopt one of the methods proposed by Danielsson *et al.* (2016). It chooses k that minimizes the “Kolmogorov-Smirnov” (KS) distance between the empirical tail and the theoretical tail of a Pareto distribution, which is shown in their paper to exhibit relatively good/stable performance in finite samples. This method is implemented by the function `mindist` of the R package `tea`.

We now report empirical biases (average minus theoretical value) and standard errors computed as sample standard deviations. For $\alpha = 2.1$, the results with $k = 2\lfloor N^{1/2} \rfloor$ are presented in Table 2, and the results with the optimal k s based on the KS method in Table 3. We put the results with the KS method when $\alpha \in \{3, 4, 5\}$ in Section D of Appendix since they show similar results as when $\alpha = 2.1$. The conclusions are summarized as follows.

1. The estimator is consistent as both the bias and the standard errors decrease with increasing sample sizes, across almost all values of ρ_{XY} . The data-driven method for selecting k yields slightly higher standard errors than the deterministic method, but it produces relatively smaller biases when $|\rho_{XY}|$ is close to 1.
2. The bias tends to increase in magnitude as $|\rho_{XY}|$ approaches 1. This could be due

to the effect of the boundary, $\rho_{XY} \in \{-1, 1\}$. These barriers make the estimator underestimate the true value.

3. The standard errors are observed to be non-uniform across ρ_{XY} , they roughly behave like a quadratic function of ρ_{XY} with its peak at ± 0.5 .

The last finding suggests that the asymptotic variance of $\hat{\rho}_{n,k}$ could be proportional to $|\rho_{XY}|(1 - |\rho_{XY}|)$, just like for the classic correlation coefficient. The derivation of the asymptotic distribution of $\hat{\rho}_{XY}$ is postponed to future work.

6 Applications to financial and climate data

In this section, we compute the extremal correlation coefficient for a number of paired functional data samples that fall into two categories: intraday returns and daily temperatures. Our objective is to show that the coefficient provides meaningful and useful information.

6.1 Extremal dependence of intraday returns on sector ETFs

In this section, we study pairwise extremal dependence of cumulative intraday return curves (CIDRs) of Exchange Traded Funds (ETFs) reflecting performance of key sectors of the U.S. economy. We work with nine Standard & Poor's Depository Receipt ETFs listed in Table 4. Our objective is to measure the tendency of paired CIDRs to exhibit similar extreme daily trajectories during the market decline caused by the COVID-19 pandemic. The CIDRs are defined as follows. Denote by $P_i(t)$ the price of an asset on trading day i at time t . For the assets in our example, t is time in minutes between 9:30 and 16:00 EST (NYSE opening times) rescaled to the unit interval $(0, 1)$. The CIDR on day i is the curve

$$R_i(t) = \ln P_i(t) - \ln P_i(0), \quad t \in [0, 1],$$

where $P_i(0)$ is the opening price on day i . The curves R_i show how the return accumulates over the trading day, see Figure 2. We consider all full trading days between Jan 02, 2020 and July 31, 2020 ($N = 147$).

Recall that the mathematical framework (3.1) from which ρ_{XY} is derived assumes that the marginal distributions of X and Y are tail equivalent. Using the estimates $\hat{\alpha}$ in Table 4 and a power transformation, we standardize all tails to $\alpha = 2.5$. For completeness, we recall this method. Given $X \in RV(-\alpha_X, \Gamma_X)$ and $Y \in RV(-\alpha_Y, \Gamma_Y)$, consider the transformation

$$g_X(x) = \frac{x}{\|x\|^{1-\alpha_X/\alpha}}, \quad g_Y(y) = \frac{y}{\|y\|^{1-\alpha_Y/\alpha}}, \quad x, y \in L^2,$$

Table 4: The nine sector ETFs and the estimates $\hat{\alpha}$ computed by applying the Hill estimator to $\|R_i\|$ with the function `mindist` of the R package `tea`.

Ticker	Sector	$\hat{\alpha}$
XLY	Consumer Discretionary	3.8
XLP	Consumer Staples	2.6
XLE	Energy	4.2
XLF	Financials	4.0
XLV	Health Care	3.9
XLI	Industrials	3.7
XLB	Materials	3.4
XLK	Technology	4.7
XLU	Utilities	3.8

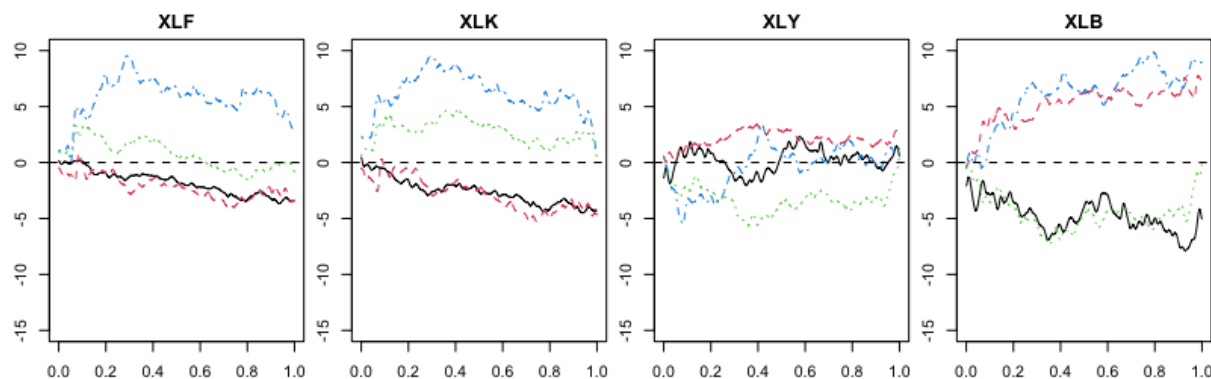


Figure 2: The CIDR of four ETFs on the four most extreme days during the Covid-19 market decline. Curves of matching color and type represent curves on the same day; XLF is paired with XLK and XLY with XLB.

where α is a desired tail index. Applying g_X and g_Y to X and Y , respectively, makes them tail equivalent because $P(\|g_X(X)\| > \cdot)$ and $P(\|g_Y(Y)\| > \cdot)$ are regularly varying with $-\alpha$. Since this method adjusts only the scale of curves, the transformed curves still retain their original shapes. After applying the above transform, we select an optimal k for each pair using the KS method described in Section 5 to compute $\hat{\rho}_{n,k}$.

Figure 3 shows estimates of the pairwise *extremal correlation coefficient* across the nine ETF sectors. All pairs exhibit positive extremal correlations ($\hat{\rho}_{n,k} = 0.39 \sim 0.96$), and 56% of the pairs have strong extremal correlations above 0.7. We see that the CIDRs overall exhibit matching patterns of cumulative intraday returns on extreme market volatility days during the Covid-19 market turbulence. To the first approximation, on such days, almost all sectors drop together or increase together. However, our coefficient reveals more

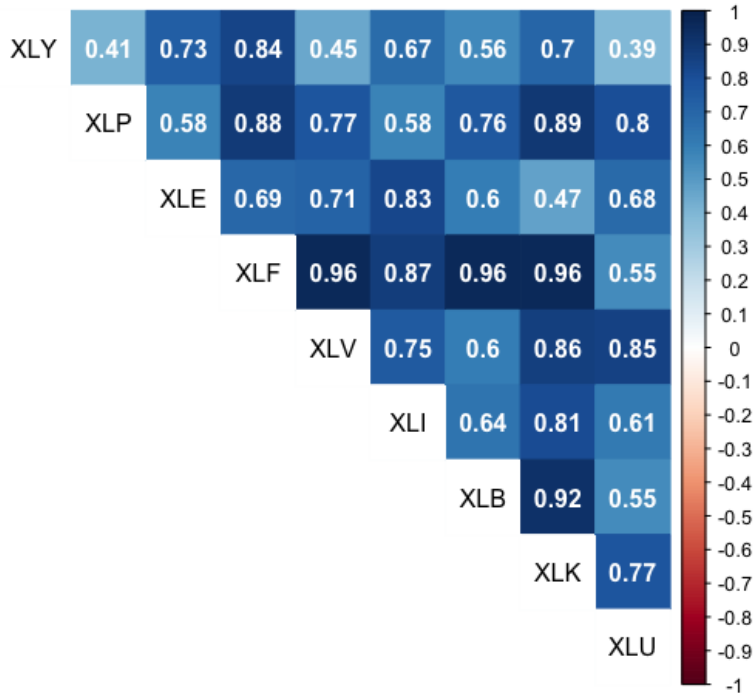


Figure 3: Estimates of the pairwise extremal correlation coefficients of CIDRs across the nine sectors.

subtle information as well. For example, extreme return curves of XLF (Financials) are exceptionally strongly correlated with extreme curves for XLV, XLB and XLK (Health Care, Materials, Technology), but relatively weakly correlated with XLU (Utilities). We use this example for illustration and do not aim at an analysis of the stock market or the economy, but we note that some findings are interesting. One might expect that the financial sector (mostly banks) will be strongly affected by the technology sector (mostly large IT companies like Google or Microsoft) because such mega corporations dominate the U.S. stock market. The similarity of extreme return curves for XLF and XLK is illustrated in the two left panels of Figure 2. One could also expect that the stocks of banks will be less affected by the performance of utility companies whose revenues are to a large extent fixed. But it is less obvious that banks are strongly correlated with Health Care and Materials sectors. As another comparison, consider XLY (Consumer Discretionary) and XLB (Materials) that show a weak extremal correlation, $\hat{\rho}_{n,k} = 0.39$. Their extreme curves exhibit dissimilar patterns, see the right two panels in Figure 2.

6.2 Extremal correlation between daily temperature curves

In this section, we evaluate the tendency of paired daily temperature curves to exhibit similar extreme patterns across three locations in the United States. The three locations

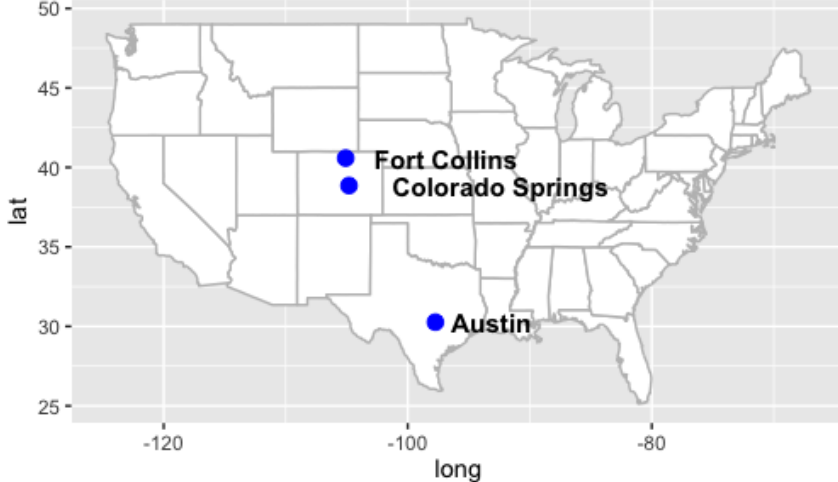


Figure 4: The three locations in the United States: Fort Collins, CO; Colorado Springs, CO; Austin, TX. The pairwise extremal correlation of daily temperature curves between the three locations is evaluated.

are marked in Figure 4. We focus on the pairwise extremal dependence of those curves during the 2021 heat wave. Although this example focuses on temperature curves, our tool can be used for analyzing other curves during extreme weather events; for example, daily precipitation patterns or river flows during floods. A correlation of extreme data during past events may help with planning a resilient infrastructure that can better withstand the next extreme weather event.

We use hourly temperature measurements provided by the European Centre for Medium-Range Weather Forecasts (ECMWF). The data are part of their ERA5 (Fifth Generation of ECMWF atmospheric reanalyses) dataset, and represent the temperatures of air at 2 meters above the surface of land, sea or inland waters. We refer to Hersbach *et al.* (2020) for more details on the ERA5 data. We partition the hourly data into daily curves, with each day’s curve beginning at UTC+0, to produce concurrent daily temperature curves across locations in different time zones. We denote the temperature (in Celsius) on day i at hour t and at location $s \in \{\text{Fort Collins, Colorado Springs, Austin}\}$ by $X_i(s, t)$, $i = 1, \dots, N$. Figure 5 depicts examples of daily temperature curves at the three locations. The data are taken from May 17, 2021 to Aug 31, 2021 ($N = 107$).

Prior to computing $\hat{\rho}_{n,k}$ for each pair of the three locations, daily curves are centered by the mean function, $\bar{X}_N(s, t) = \frac{1}{N} \sum_{i=1}^N X_i(s, t)$, for each location s . We then compute the tail index estimate $\hat{\alpha}$ of the norms $\|X_i(s, t) - \bar{X}_N(s, t)\|$, for each location s , shown in Table 5. The results suggest that the marginal distributions of those curves across the three locations are not tail-equivalent. We apply the power transformation method, described in Section 6.1, to get the tail index $\alpha = 2.5$ at all locations. We then apply the

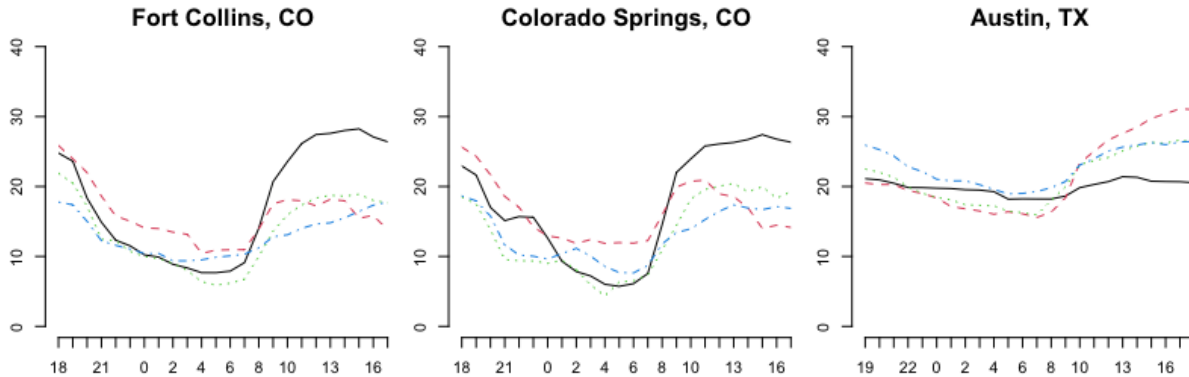


Figure 5: Extreme daily temperature curves (in Celsius) during the 2021 heat wave (local time on the x-axis). Curves of matching color represent the same days when both Fort Collins and Colorado Springs experienced extreme patterns simultaneously.

Table 5: Tail index estimates $\hat{\alpha}$ and estimates of the pairwise extremal correlation coefficients, $\hat{\rho}_{n,k}$, of daily temperature curves across Fort Collins, CO, Colorado Springs, CO, and Austin, TX.

Location	$\hat{\alpha}$	$\hat{\rho}_{n,k}$		
		Fort Collins	Colorado Springs	Austin
Fort Collins	5.5	1	0.94	0.79
Colorado Springs	3.6	0.94	1	0.74
Austin	4.4	0.79	0.74	1

KS method, described in Section 5, to the centered curves to select an optimal k for each pair.

Table 5 reports estimates of the pairwise *extremal correlation coefficient* across the three locations. There are positive and strong extremal correlations among all pairs ($\hat{\rho}_{n,k} = 0.74 \sim 0.94$), suggesting a high degree of association between the daily temperature extreme patterns across the three locations, even between different climatic regions like the Front Range foothills and the southern edge of the Great Plains. We see that the proximity in geographical locations corresponds to greater similarity in extreme patterns, showing that $\hat{\rho}_{n,k}$ is a meaningful and useful dependence measure.

Acknowledgements

We Thank Professor Hong Miao of the Department of Finance and Real Estate at Colorado State University for preprocessing the financial data used in Section 6.1. We thank Professor Joshua French of the Department of Mathematical and Statistical Sciences at the University of Colorado Denver for preprocessing the temperature data used in Section

6.2.

Conflicts of interest: None declared.

Funding

P.K. was partially supported by the United States National Science Foundation grant DMS–2123761.

Data availability

The raw high frequency financial data used in Section 6.1 can be acquired from tick-data.com, as well as from many other providers. The reanalysis temperature data used in Section 6.2 can be downloaded from ecmwf.int. The R code used in this paper can be found at github.com/veritasmih/ecc.

Supplementary material

Supplementary material is available at Journal of the Royal Statistical Society: Series B online

References

- Billingsley, P. (1999). *Convergence of Probability Measures; Second Edition*. Wiley, New York.
- Cléménçon, S., Huet, N. and Sabourin, A. (2024). Regular variation in Hilbert spaces and principal component analysis for functional extremes. *Stochastic Processes and their Applications*; forthcoming.
- Danielsson, J., Ergun, L. M., de Haan, L. and de Vries, C. G. (2016). Tail index estimation: Quantile driven threshold selection. Technical Report. Bank of Canada.
- Danielsson, J., de Haan, L., Peng, L. and de Vries, C.G. (2001). Using a bootstrap method to choose the sample fraction in tail index estimation. *Journal of Multivariate Analysis*, **76**.
- Davis, R. A. and Mikosch, T. (2009). The extremogram: A correlogram for extreme events. *Bernoulli*, **15**, 977–1009.
- de Haan, L. and Ferreira, A. (2000). *Extreme Value Theory*. Springer.
- Dombry, C. and Ribatet, M. (2015). Functional regular variations, Pareto processes and peaks over threshold. *Statistics and its Interface*, **8**, 9–17.
- Drees, H. and Kaufmann, E. (1998). Selecting the optimal sample fraction in univariate extreme value estimation. *Stochastic Processes and their Applications*, **75**, 149–172.
- Dubin, J. A. and Müller, H. G. (2005). Dynamical correlation for multivariate longitudinal data. *Journal of the American Statistical Association*, **100**, 872–881.
- Hall, P. (1990). Using the bootstrap to estimate mean squared error and select smoothing parameter in nonparametric problems. *Journal of Multivariate Analysis*, **32**, 177–203.

- Hall, P. and Welsh, A. H. (1985). Adaptive estimates of parameters of regular variation. *The Annals of Statistics*, **13**, 331–341.
- Hersbach, H., Bell, B., Berrisford, P., Hirahara, S., Horányi, A., Muñoz-Sabater, J., Nicolas, J., Peubey, C., Radu, R., Schepers, D. *et al.* (2020). The ERA5 global reanalysis. *Quarterly Journal of the Royal Meteorological Society*, **146**, 1999–2049.
- Hsing, T. and Eubank, R. (2015). *Theoretical Foundations of Functional Data Analysis, with an Introduction to Linear Operators*. Wiley.
- Hult, H. and Lindskog, F. (2006). Regular variation for measures on metric spaces. *Publications de l’Institut Mathématique. Nouvelle Série*, **80(94)**, 121–140.
- Janßen, A., Neblung, S. and Stoev, S. (2023). Tail-dependence, exceedance sets, and metric embeddings. *Extremes*, 1–39.
- Kim, M. and Kokoszka, P. (2019). Hill estimator of projections of functional data on principal components. *Statistics*, **53**, 699–720.
- Kim, M. and Kokoszka, P. (2022). Extremal dependence measure for functional data. *Journal of Multivariate Analysis*, **189**, 104887.
- Kokoszka, P. and Kulik, R. (2023). Principal component analysis of infinite variance functional data. *Journal of Multivariate Analysis*, **193**, 105123.
- Kokoszka, P. and Reimherr, M. (2017). *Introduction to Functional Data Analysis*. CRC Press.
- Kokoszka, P., Stoev, S. and Xiong, Q. (2019). Principal components analysis of regularly varying functions. *Bernoulli*, **25**, 3864–3882.
- Kokoszka, P. and Xiong, Q. (2018). Extremes of projections of functional time series on data-driven basis systems. *Extremes*, **21**, 177–204.
- Larsson, M. and Resnick, S. I. (2012). Extremal dependence measure and extremogram: the regularly varying case. *Extremes*, **15**, 231–256.
- Ledford, A. W. and Tawn, J. A. (1996). Statistics for near independence in multivariate extreme values. *Biometrika*, **83**, 169–187.
- Ledford, A. W. and Tawn, J. A. (1997). Modelling dependence within joint tail regions. *Journal of the Royal Statistical Society: Series B (Statistical Methodology)*, **59**, 475–499.
- Ledford, A. W. and Tawn, J. A. (2003). Diagnostics for dependence within time series extremes. *Journal of the Royal Statistical Society: Series B (Statistical Methodology)*, **65**, 521–543.
- McDiarmid, C. (1998). Concentration. In *Probabilistic Methods for Algorithmic Discrete Mathematics*, pp. 195–248. Springer.
- Meiguet, T. (2010). Heavy Tailed Functional Time Series. Ph.D. Thesis. Université catholique de Louvain.
- Resnick, S. I. (1987). *Extreme Values, Regular Variation, and Point Processes*. Springer.
- Resnick, S. I. (2004). The extremal dependence measure and asymptotic independence. *Stochastic models*, **20**, 205–227.

Resnick, S. I. (2007). *Heavy-Tail Phenomena*. Springer.

Yeh, C. K., Rice, G. and Dubin, J. A. (2023). Functional spherical autocorrelation: A robust estimate of the autocorrelation of a functional time series. *Electronic Journal of Statistics*, **17**, 650–687.

Supplementary Material

A Preliminary results

In this section, we put together preliminary results needed to prove Theorem 4.1. These results allow us to streamline the exposition of proofs of the main result. Recall that, c.f., (3.2), $\mathcal{A}_r = \{(x, y) \in \mathbb{B}_0^2 : \|(x, y)\|_{\mathbb{B}^2} \geq r\}$, $r > 0$, where $\|(x, y)\|_{\mathbb{B}^2} = \|x\|_{\mathbb{B}} \vee \|y\|_{\mathbb{B}}$.

LEMMA A.1 *Suppose μ is a measure in $M_0(\mathbb{B}^2)$ satisfying $\mu(t \cdot) = t^{-\alpha} \mu(\cdot)$, $t > 0$. Then, \mathcal{A}_r is a μ -continuity set, i.e., $\mu(\partial \mathcal{A}_r) = 0$.*

PROOF: We assume $\mu(\partial \mathcal{A}_r) > 0$ and get a contradiction. Since $\mathcal{A}_r \supset \bigcup_{n \geq 1} \partial(n^{1/\alpha} \mathcal{A}_r)$, it follows from the homogeneity property of μ that

$$\mu(\mathcal{A}_r) \geq \sum_{n=1}^{\infty} \mu(\partial(n^{1/\alpha} \mathcal{A}_r)) = \sum_{n=1}^{\infty} \mu(n^{1/\alpha} \partial \mathcal{A}_r) = \sum_{n=1}^{\infty} n^{-1} \mu(\partial \mathcal{A}_r) = \infty.$$

It contradicts to the fact that μ is *boundedly finite*. ■

Recall that $R = \|(X, Y)\|$, $R_i = \|(X_i, Y_i)\|$, and $R_{(k)}$ is the k th largest order statistic with the convention $R_{(1)} = \max\{R_1, \dots, R_n\}$. Let $b(n)$ be the quantile function such that $P(R > b(n)) = n^{-1}$. We claim in the following lemma that regular variation of $[X, Y]^\top$ in $L^2 \times L^2$ implies regular variation of R in $[0, \infty)$.

LEMMA A.2 *Let $M_+(0, \infty]$ be the space of Radon measures on $(0, \infty]$, and $\nu_\alpha(r, \infty] = r^{-\alpha}$. If $[X, Y]^\top$ is regularly varying in $L^2 \times L^2$ according to Definition 3.1, then*

(i) R is a nonnegative random variable whose distribution has a regularly varying tail with index $-\alpha$,

(ii) $\frac{1}{k} \sum_{i=1}^n I_{R_i/b(n/k)} \xrightarrow{P} \nu_\alpha$, in $M_+(0, \infty]$,

(iii) $R_{(k)}/b(n/k) \xrightarrow{P} 1$, in $[0, \infty)$,

(iv) $\frac{1}{k} \sum_{i=1}^n I_{R_i/R_{(k)}} \xrightarrow{P} \nu_\alpha$ in $M_+(0, \infty]$.

PROOF: For statement (i), observe that for $r > 0$,

$$\frac{n}{k} P(R \geq rb(n/k)) = \frac{n}{k} P\left(\frac{(X, Y)}{b(n/k)} \in \mathcal{A}_r\right),$$

where \mathcal{A}_r is defined in (3.2). It then follows from (3.1) and (3.3) that

$$\frac{n}{k} P(R \geq rb(n/k)) \rightarrow \mu(\mathcal{A}_r) = r^{-\alpha} \mu(\mathcal{A}_1) = r^{-\alpha}.$$

Therefore, by Theorem 3.6 of Resnick (2007), (i) holds. By Theorem 4.1 of Resnick (2007), it can be shown that (i) implies (ii). Also, it follows from Step 1 in the proof of Theorem 4.2 of Resnick (2007) that (ii) implies (iii) and from Step 2 in that proof that (ii) and (iii) imply (iv). ■

The following lemma is used to prove Lemmas A.4 and A.5.

LEMMA A.3 *Suppose γ_n converges vaguely to ν_α in $M_+(0, \infty]$. Then for any compact interval $K \subset (0, \infty]$,*

$$\int_K r^2 \gamma_n(dr) \rightarrow \int_K r^2 \nu_\alpha(dr).$$

PROOF: Since the function $r \mapsto r^2 I_K$ is not continuous, we use an approximation argument. Set $K = [a, b]$, for $0 < a < b \leq \infty$. Construct compact intervals $K_j \searrow K$ and nonnegative continuous functions f_j such that $I_K \leq f_j \leq I_{K_j}$. By the triangle inequality,

$$\begin{aligned} \left| \int_K r^2 \gamma_n(dr) - \int_K r^2 \nu_\alpha(dr) \right| &\leq \left| \int r^2 I_K(r) \gamma_n(dr) - \int r^2 f_j(r) \gamma_n(dr) \right| \\ &\quad + \left| \int r^2 f_j(r) \gamma_n(dr) - \int r^2 f_j(r) \nu_\alpha(dr) \right| \\ &\quad + \left| \int r^2 f_j(r) \nu_\alpha(dr) - \int r^2 I_K(r) \nu_\alpha(dr) \right| \\ &=: A_{n,j}^{(1)} + A_{n,j}^{(2)} + A_j^{(3)}. \end{aligned}$$

Fix $\epsilon > 0$. There is j^* such that for $j \geq j^*$,

$$A_j^{(3)} \leq c \int [f_j(r) - I_K(r)] \nu_\alpha(dr) \leq c \nu_\alpha(K_j \setminus K^\circ) < \epsilon/2,$$

where $c = b^2 I_{b \neq \infty} + a^2 I_{b = \infty}$. Similarly $A_{n,j}^{(1)} \leq c \gamma_n(K_j \setminus K^\circ)$, so for every fixed j ,

$$\limsup_{n \rightarrow \infty} A_{n,j}^{(1)} \leq M^2 \limsup_{n \rightarrow \infty} \gamma_n(K_j \setminus K^\circ) \leq M^2 \nu_\alpha(K_j \setminus K^\circ)$$

because $K_j \setminus K^\circ$ is compact, cf. Proposition 3.12 in Resnick (1987). Thus,

$$\limsup_{n \rightarrow \infty} \left| \int_K r^2 \gamma_n(dr) - \int_K r^2 \nu_\alpha(dr) \right| \leq \epsilon + \limsup_{n \rightarrow \infty} A_{n,j^*}^{(2)} = \epsilon.$$

Since ϵ is arbitrary, we get the claim. ■

The following two lemmas are used to prove Lemma A.6 and Proposition B.1.

LEMMA A.4 *Under Assumption 4.1, for any $M > 0$,*

$$\frac{n}{k} E \left[\left(\frac{R}{b(n/k)} \right)^2 I_{R \geq Mb(n/k)} \right] \rightarrow \frac{\alpha}{\alpha - 2} M^{2-\alpha}.$$

PROOF: Observe that

$$\frac{n}{k} E \left[\left(\frac{R}{b(n/k)} \right)^2 I_{R \geq Mb(n/k)} \right] = \int_M^\infty r^2 \frac{n}{k} P \left(\frac{R}{b(n/k)} \in dr \right),$$

and

$$\frac{\alpha}{\alpha - 2} M^{2-\alpha} = \int_M^\infty r^2 \nu_\alpha(dr).$$

By Lemma A.2 (i), we have that in $M_+(0, \infty]$

$$\frac{n}{k} P \left(\frac{R}{b(n/k)} \in \cdot \right) \xrightarrow{v} \nu_\alpha.$$

Therefore, we get the claim by Lemma A.3 with $K = [M, \infty]$. ■

LEMMA A.5 *The function h on $M_+(0, \infty]$ defined by $h(\gamma) = \int_1^M r^2 \gamma(dr)$ is continuous at ν_α .*

PROOF: Suppose γ_n converges vaguely to ν_α . Then, by Lemma A.3 with $K = [1, M]$, it can be shown that

$$\lim_{n \rightarrow \infty} \int_1^M r^2 \gamma_n(dr) = \int_1^M r^2 \nu_\alpha(dr).$$
■

The following lemma is the key argument to prove Proposition B.2.

LEMMA A.6 *Under Assumption 4.1, the following statements hold:*

$$(A.1) \quad \frac{1}{k} \sum_{i=1}^n \left(\frac{R_i}{R_{(k)}} \right)^2 I_{R_i \geq R_{(k)}} \xrightarrow{P} \frac{\alpha}{\alpha - 2};$$

$$(A.2) \quad \frac{1}{k} \sum_{i=1}^n \left(\frac{R_i}{b(n/k)} \right)^2 I_{R_i \geq b(n/k)} \xrightarrow{P} \frac{\alpha}{\alpha - 2}.$$

PROOF: The proofs for (A.1) and (A.2) are almost the same, so we only prove (A.1) to save space. Let $\hat{\gamma}_{n,k} = \frac{1}{k} \sum_{i=1}^n I_{R_i/R_{(k)}}$, and recall that $\hat{\gamma}_{n,k} \xrightarrow{P} \nu_\alpha$ (see Lemma A.2 (iv)). Since

$$\frac{1}{k} \sum_{i=1}^n \left(\frac{R_i}{R_{(k)}} \right)^2 I_{R_i \geq R_{(k)}} = \int_1^\infty r^2 \hat{\gamma}_{n,k}(dr),$$

we need to show that

$$\int_1^\infty r^2 \hat{\gamma}_{n,k}(dr) \xrightarrow{P} \int_1^\infty r^2 \nu_\alpha(dr) = \frac{\alpha}{\alpha - 2}.$$

To prove this convergence, we use the second converging together theorem, Theorem 3.5 in Resnick (2007), (also stated as Theorem 3.2 of Billingsley (1999)). Let

$$\begin{aligned} V_{n,k} &= \int_1^\infty r^2 \hat{\gamma}_{n,k}(dr), & V &= \int_1^\infty r^2 \nu_\alpha(dr); \\ V_{n,k}^{(M)} &= \int_1^M r^2 \hat{\gamma}_{n,k}(dr), & V^{(M)} &= \int_1^M r^2 \nu_\alpha(dr). \end{aligned}$$

To show the desired convergence $V_{n,k} \xrightarrow{P} V$ (equivalently, $V_{n,k} \xrightarrow{d} V$), we must verify that

$$(A.3) \quad \forall M > 1, \quad V_{n,k}^{(M)} \xrightarrow{d} V^{(M)}, \quad \text{as } n \rightarrow \infty;$$

$$(A.4) \quad V^{(M)} \xrightarrow{d} V, \quad \text{as } M \rightarrow \infty;$$

$$(A.5) \quad \forall \varepsilon > 0, \quad \lim_{M \rightarrow \infty} \limsup_{n \rightarrow \infty} P\left(|V_{n,k}^{(M)} - V_{n,k}| > \varepsilon\right) = 0.$$

Convergence (A.3) follows from Lemma A.2 (iv) and Lemma A.5. Convergence (A.4) holds since for $\alpha > 2$

$$\int_M^\infty r^2 \nu_\alpha(dr) = \int_M^\infty r^2 \alpha r^{-\alpha-1} dr = \frac{\alpha}{\alpha-2} M^{2-\alpha} \rightarrow 0, \quad \text{as } M \rightarrow \infty.$$

It remains to show that $\forall \varepsilon > 0$,

$$\lim_{M \rightarrow \infty} \limsup_{n \rightarrow \infty} P\left(|V_{n,k}^{(M)} - V_{n,k}| > \varepsilon\right) = \lim_{M \rightarrow \infty} \limsup_{n \rightarrow \infty} P\left(\int_M^\infty r^2 \hat{\gamma}_{n,k}(dr) > \varepsilon\right) = 0.$$

Fix $\varepsilon > 0$ and $\eta > 0$. Observe that

$$P\left(\int_M^\infty r^2 \hat{\gamma}_{n,k}(dr) > \varepsilon\right) \leq Q_1(n) + Q_2(n),$$

where

$$Q_1(n) = P\left(\int_M^\infty r^2 \hat{\gamma}_{n,k}(dr) > \varepsilon, \left|\frac{R(k)}{b(n/k)} - 1\right| < \eta\right), \quad Q_2(n) = P\left(\left|\frac{R(k)}{b(n/k)} - 1\right| \geq \eta\right).$$

By Lemma A.2 (iii), $\limsup_{n \rightarrow \infty} Q_2(n) = 0$. For $Q_1(n)$, we start with the bound

$$\begin{aligned} Q_1(n) &\leq P\left(\int_M^\infty r^2 \hat{\gamma}_{n,k}(dr) > \varepsilon, \frac{R(k)}{b(n/k)} > 1 - \eta\right) \\ &= P\left(\int_M^\infty r^2 \frac{1}{k} \sum_{i=1}^n I_{R_i/R(k) \in dr} > \varepsilon, \frac{R(k)}{b(n/k)} > 1 - \eta\right). \end{aligned}$$

Conditions $R_i/R_{(k)} > M$ and $R_{(k)}/b(n/k) > 1 - \eta$ imply $R_i/b(n/k) > M(1 - \eta)$, so

$$\begin{aligned} Q_1(n) &\leq P \left(\int_{M(1-\eta)}^{\infty} r^2 \frac{1}{k} \sum_{i=1}^n I_{R_i/b(n/k) \in dr} > \varepsilon \right) \\ &= P \left(\frac{1}{k} \sum_{i=1}^n \left(\frac{R_i}{b(n/k)} \right)^2 I_{R_i \geq M(1-\eta)b(n/k)} > \varepsilon \right). \end{aligned}$$

Then, it follows from Markov's inequality and Lemma A.4 that

$$Q_1(n) \leq \frac{1}{\varepsilon} \frac{n}{k} E \left[\left(\frac{R_1}{b(n/k)} \right)^2 I_{R_1 \geq M(1-\eta)b(n/k)} \right] \rightarrow \frac{1}{\varepsilon} \frac{\alpha}{\alpha - 2} \{M(1 - \eta)\}^{2-\alpha}, \quad \text{as } n \rightarrow \infty.$$

This bound goes to 0 as $M \rightarrow \infty$ since $\alpha > 2$. ■

The following lemma follows from Theorem 3.8 of McDiarmid (1998). It states a Bernstein type inequality, which is the key technique to prove Proposition B.1.

LEMMA A.7 *Let $\mathbf{Z}_n = (Z_1, \dots, Z_n)$ with the Z_i taking values in a Lebesgue measurable subset \mathcal{Z} of an Euclidean space. Let f be a real-valued function defined on \mathcal{Z}^n . For $(z_1, \dots, z_i) \in \mathcal{Z}^i$, $1 \leq i \leq n$, put*

$$(A.6) \quad g_i(z_1, \dots, z_i) := E[f(\mathbf{Z}_n) | Z_j = z_j, 1 \leq j \leq i] - E[f(\mathbf{Z}_n) | Z_j = z_j, 1 \leq j \leq i-1].$$

Define the maximum deviation by

$$(A.7) \quad b := \max_{1 \leq i \leq n} \sup_{(z_1, \dots, z_i) \in \mathcal{Z}^i} g_i(z_1, \dots, z_i),$$

and define the supremum sum of variances by

$$(A.8) \quad \hat{v} := \sup_{(z_1, \dots, z_n) \in \mathcal{Z}^n} \sum_{i=1}^n \text{Var}[g_i(z_1, \dots, z_{i-1}, Z'_i)],$$

where Z'_i is an independent copy of Z_i conditional on $Z_j = z_j$, $1 \leq j \leq i-1$. If b and \hat{v} are finite, then for any $\varepsilon \geq 0$,

$$P(f(\mathbf{Z}_n) - E[f(\mathbf{Z}_n)] \geq t) \leq \exp\left(\frac{-\varepsilon^2}{2(\hat{v} + b\varepsilon/3)}\right).$$

B Proof of Theorem 4.1 in Section 4

Recall (4.4), i.e., the definition:

$$\hat{\sigma}_{n,k} = \frac{1}{k} \sum_{i=1}^n \left\langle \frac{X_i}{R_{(k)}}, \frac{Y_i}{R_{(k)}} \right\rangle I_{R_i \geq R_{(k)}}.$$

To prove the consistency of $\hat{\sigma}_{n,k}$ for the *extremal covariance* σ_{XY} , we consider the following sequence of random variables

$$(B.1) \quad \sigma_{n,k} := \frac{1}{k} \sum_{i=1}^n \left\langle \frac{X_i}{b(n/k)}, \frac{Y_i}{b(n/k)} \right\rangle I_{R_i \geq b(n/k)}.$$

Note that $\sigma_{n,k}$ is not observable since $b(\cdot)$ is unknown. However, $b(n/k)$ can be estimated by its consistent estimator $R_{(k)}$, and it can be shown that replacing $b(n/k)$ by $R_{(k)}$ ensures that the difference between $\sigma_{n,k}$ and $\hat{\sigma}_{n,k}$ is asymptotically negligible, which will be shown in Proposition B.2. Thus, the key argument for establishing the consistency is to show that $\sigma_{n,k}$ converges in probability to σ_{XY} , which is proven in the following proposition.

PROPOSITION B.1 *Under Assumption 4.1,*

$$\sigma_{n,k} \xrightarrow{P} \sigma_{XY}.$$

PROOF: Set

$$(B.2) \quad \bar{\sigma}_{n,k} := E \left[\left\langle \frac{X_1}{b(n/k)}, \frac{Y_1}{b(n/k)} \right\rangle \middle| \|X_1\| \vee \|Y_1\| > b(n/k) \right].$$

Then, by Proposition 4.1, $\bar{\sigma}_{n,k} \rightarrow \sigma_{XY}$, so it remains to show that $|\sigma_{n,k} - \bar{\sigma}_{n,k}| \xrightarrow{P} 0$.

Let $\mathbf{Z}_n = (Z_1, \dots, Z_n)$, where $Z_i = (X_i, Y_i)$, and $\mathbf{z}_n = (z_1, \dots, z_n)$, where $z_i = (x_i, y_i)$, for $1 \leq i \leq n$. Consider a map $f : (L^2 \times L^2)^n \rightarrow \mathbb{R}$ defined by

$$f(\mathbf{z}_n) := \left| \frac{1}{k} \sum_{i=1}^n \left\langle \frac{x_i}{b(n/k)}, \frac{y_i}{b(n/k)} \right\rangle I_{r_i \geq b(n/k)} - \frac{n}{k} E \left[\left\langle \frac{X_1}{b(n/k)}, \frac{Y_1}{b(n/k)} \right\rangle I_{R_1 > b(n/k)} \right] \right|.$$

Then, we have that

$$|\sigma_{n,k} - \bar{\sigma}_{n,k}| = f(\mathbf{Z}_n) - E[f(\mathbf{Z}_n)] + E[f(\mathbf{Z}_n)].$$

We aim to show that $f(\mathbf{Z}_n) - E[f(\mathbf{Z}_n)] \xrightarrow{P} 0$ and $E[f(\mathbf{Z}_n)] \rightarrow 0$.

To establish the convergence, $f(\mathbf{Z}_n) - E[f(\mathbf{Z}_n)] \xrightarrow{P} 0$, we use the Bernstein type concentration inequality in Lemma A.7. Since the (X_i, Y_i) are independent, the deviation function in (A.6) has the following form

$$g_i(z_1, \dots, z_i) = E[f(z_1, \dots, z_{i-1}, z_i, Z_{i+1}, \dots, Z_n) - f(z_1, \dots, z_{i-1}, Z_i, Z_{i+1}, \dots, Z_n)].$$

Then, using the fact that $\|x\| - \|y\| \leq \|x - y\|$, we have that

$$\begin{aligned} g_i(z_1, \dots, z_i) &\leq \frac{1}{k} E \left[\left| \left\langle \frac{x_i}{b(n/k)}, \frac{y_i}{b(n/k)} \right\rangle I_{r_i \geq b(n/k)} - \left\langle \frac{X_i}{b(n/k)}, \frac{Y_i}{b(n/k)} \right\rangle I_{R_i \geq b(n/k)} \right| \right] \\ &\leq \frac{1}{k} \left\{ \frac{\|x_i\| \|y_i\|}{b(n/k)^2} + \frac{k}{n} E \left[\left(\frac{R_i}{b(n/k)} \right)^2 I_{R_i \geq b(n/k)} \right] \right\} \\ &\leq \frac{1}{k} \left\{ \frac{\|x_i\| \|y_i\|}{b(n/k)^2} + \frac{n}{k} E \left[\left(\frac{R_i}{b(n/k)} \right)^2 I_{R_i \geq b(n/k)} \right] \right\}. \end{aligned}$$

Since $(x_i, y_i) \in L^2 \times L^2$ and $\frac{n}{k}E[(R_i/b(n/k))^2 I_{R_i \geq b(n/k)}] \rightarrow \alpha/(\alpha - 2)$ by Lemma A.4, we have that $g_i(z_1, \dots, z_i) \leq c_1/k$, for some constant $c_1 > 0$. Therefore, the maximum deviation b in (A.7) is bounded by c_1/k .

Next we investigate the upper bound for the sum of variances \hat{v} in (A.8). Since $E[g_i(z_1, \dots, z_{i-1}, Z'_i)] = 0$ by the law of total probability, we have that

$$\begin{aligned} & \text{Var}[g_i(z_1, \dots, z_{i-1}, Z'_i)] \\ &= E[g_i^2(z_1, \dots, z_{i-1}, Z'_i)] \\ &= E\left[\left\{f(z_1, \dots, z_{i-1}, Z'_i, Z_{i+1}, \dots, Z_n) - f(z_1, \dots, z_{i-1}, Z_i, Z_{i+1}, \dots, Z_n)\right\}^2\right] \\ &\leq \frac{1}{k^2}E\left[\left\{\left\langle \frac{X'_i}{b(n/k)}, \frac{Y'_i}{b(n/k)} \right\rangle I_{R'_i \geq b(n/k)} - \left\langle \frac{X_i}{b(n/k)}, \frac{Y_i}{b(n/k)} \right\rangle I_{R_i \geq b(n/k)}\right\}^2\right] \\ &\leq \frac{2}{k^2}E\left[\left\langle \frac{X_i}{b(n/k)}, \frac{Y_i}{b(n/k)} \right\rangle^2 I_{R_i \geq b(n/k)}\right] \\ &\leq \frac{2}{k^2}\left\{\frac{k}{n}\frac{n}{k}E\left[\left(\frac{R_i}{b(n/k)}\right)^2 I_{R_i \geq b(n/k)}\right]\right\}. \end{aligned}$$

It then again follows from Lemma A.4 that $\text{Var}[g_i(z_1, \dots, z_{i-1}, Z'_i)] \leq c_2/(nk)$ for some $c_2 > 0$. Then the supremum sum of variances \hat{v} is bounded above by c_2/k . Therefore by Lemma A.7, for any $\varepsilon > 0$

$$P(f(\mathbf{Z}_n) - E[f(\mathbf{Z}_n)] \geq \varepsilon) \leq \exp\left(\frac{-k\varepsilon^2}{c_1 + c_2\varepsilon/3}\right).$$

If we apply this inequality to $-f(\mathbf{Z}_n)$, then we obtain the following ‘two-sided’ inequality

$$P(|f(\mathbf{Z}_n) - E[f(\mathbf{Z}_n)]| \geq \varepsilon) \leq 2 \exp\left(\frac{-k\varepsilon^2}{c_1 + c_2\varepsilon/3}\right).$$

From this, we obtain that $f(\mathbf{Z}_n) - E[f(\mathbf{Z}_n)] \xrightarrow{P} 0$.

Next, to show $E[f(\mathbf{Z}_n)] \rightarrow 0$, we set, for $1 \leq i \leq n$

$$\Delta_i = \left\langle \frac{X_i}{b(n/k)}, \frac{Y_i}{b(n/k)} \right\rangle I_{R_i \geq b(n/k)} - E\left[\left\langle \frac{X_1}{b(n/k)}, \frac{Y_1}{b(n/k)} \right\rangle I_{R_1 > b(n/k)}\right].$$

Then, we have that

$$\begin{aligned} E[f(\mathbf{Z}_n)] &= \frac{n}{k}E\left[\left[\frac{1}{n}\sum_{i=1}^n \Delta_i\right]\right] \leq \frac{n}{k}\left\{E\left[\left(\frac{1}{n}\sum_{i=1}^n \Delta_i\right)^2\right]\right\}^{1/2} \\ &= \frac{n}{k}\left\{E\left[\frac{1}{n^2}\sum_{i=1}^n \Delta_i^2 + \frac{1}{n^2}\sum_{i \neq j} \Delta_i \Delta_j\right]\right\}^{1/2}. \end{aligned}$$

Since the Δ_i are independent, $E[\Delta_i \Delta_j] = 0$, for $i \neq j$. Therefore,

$$\begin{aligned}
& E[f(\mathbf{Z}_n)] \\
& \leq \frac{\sqrt{n}}{k} \{E[\Delta_1^2]\}^{1/2} \\
& = \frac{\sqrt{n}}{k} \left\{ E \left[\left(\left\langle \frac{X_1}{b(n/k)}, \frac{Y_1}{b(n/k)} \right\rangle I_{R_1 \geq b(n/k)} - E \left[\left\langle \frac{X_1}{b(n/k)}, \frac{Y_1}{b(n/k)} \right\rangle I_{R_1 \geq b(n/k)} \right] \right)^2 \right] \right\}^{1/2} \\
& = \frac{\sqrt{n}}{k} \left\{ \text{Var} \left[\left\langle \frac{X_1}{b(n/k)}, \frac{Y_1}{b(n/k)} \right\rangle I_{R_1 \geq b(n/k)} \right] \right\}^{1/2} \\
& \leq \frac{\sqrt{n}}{k} \left\{ E \left[\left\langle \frac{X_1}{b(n/k)}, \frac{Y_1}{b(n/k)} \right\rangle^2 I_{R_1 \geq b(n/k)} \right] \right\}^{1/2} \\
& \leq \frac{\sqrt{n}}{k} \left\{ E \left[\left(\frac{R_1}{b(n/k)} \right)^2 I_{R_1 \geq b(n/k)} \right] \right\}^{1/2}.
\end{aligned}$$

Therefore, by Lemma A.4 we have that

$$E[f(\mathbf{Z}_n)] \leq \frac{\sqrt{n}}{k} \left\{ \frac{k}{n} \frac{n}{k} E \left[\left(\frac{R_1}{b(n/k)} \right)^2 I_{R_1 \geq b(n/k)} \right] \right\}^{1/2} \leq \frac{c_3}{\sqrt{k}},$$

for some $c_3 > 0$, which completes the proof. ■

PROPOSITION B.2 *Under Assumption 4.1,*

$$|\hat{\sigma}_{n,k} - \sigma_{n,k}| \xrightarrow{P} 0.$$

PROOF: Consider the following decomposition

$$|\hat{\sigma}_{n,k} - \sigma_{n,k}| \leq P_1(n) + P_2(n),$$

where

$$\begin{aligned}
P_1(n) & := \left| \frac{1}{k} \sum_{i=1}^n \left\langle \frac{X_i}{R_{(k)}}, \frac{Y_i}{R_{(k)}} \right\rangle \left\{ I_{R_i \geq R_{(k)}} - I_{R_i \geq b(n/k)} \right\} \right|, \\
P_2(n) & := \left| \frac{1}{k} \sum_{i=1}^n \left\{ \left\langle \frac{X_i}{R_{(k)}}, \frac{Y_i}{R_{(k)}} \right\rangle - \left\langle \frac{X_i}{b(n/k)}, \frac{Y_i}{b(n/k)} \right\rangle \right\} I_{R_i \geq b(n/k)} \right|.
\end{aligned}$$

We will show that each of the two parts goes to 0. We first focus on $P_1(n)$. Observe that

$$\begin{aligned}
P_1(n) &\leq \left(\frac{b(n/k)}{R_{(k)}}\right)^2 \frac{1}{k} \sum_{i=1}^n \left| \left\langle \frac{X_i}{R_i}, \frac{Y_i}{R_i} \right\rangle \right| \left(\frac{R_i}{b(n/k)}\right)^2 \left| I_{R_i \geq R_{(k)}} - I_{R_i \geq b(n/k)} \right| \\
&\leq \left(\frac{b(n/k)}{R_{(k)}}\right)^2 \frac{1}{k} \sum_{i=1}^n \left(\frac{R_i}{b(n/k)}\right)^2 \left| I_{R_i \geq R_{(k)}} - I_{R_i \geq b(n/k)} \right| \\
&= \left(\frac{b(n/k)}{R_{(k)}}\right)^2 \left| \frac{1}{k} \sum_{i=1}^n \left(\frac{R_i}{b(n/k)}\right)^2 I_{R_i \geq R_{(k)}} - \frac{1}{k} \sum_{i=1}^n \left(\frac{R_i}{b(n/k)}\right)^2 I_{R_i \geq b(n/k)} \right| \\
&= \left| \frac{1}{k} \sum_{i=1}^n \left(\frac{R_i}{R_{(k)}}\right)^2 I_{R_i \geq R_{(k)}} - \left(\frac{b(n/k)}{R_{(k)}}\right)^2 \frac{1}{k} \sum_{i=1}^n \left(\frac{R_i}{b(n/k)}\right)^2 I_{R_i \geq b(n/k)} \right|
\end{aligned}$$

Then, by Lemma A.2 (iii), we have that $(b(n/k)/R_{(k)})^2 \xrightarrow{P} 1$. By Lemma A.6 that $\frac{1}{k} \sum_{i=1}^n (R_i/R_{(k)})^2 I_{R_i \geq R_{(k)}} \xrightarrow{P} \alpha/(\alpha-2)$ and $\frac{1}{k} \sum_{i=1}^n (R_i/b(n/k))^2 I_{R_i \geq b(n/k)} \xrightarrow{P} \alpha/(\alpha-2)$. Therefore, we have that $P_1(n) \xrightarrow{P} 0$.

Now we work on $P_2(n)$. Observe that

$$\begin{aligned}
P_2(n) &= \left| \frac{1}{k} \sum_{i=1}^n \left\langle \frac{X_i}{R_i}, \frac{Y_i}{R_i} \right\rangle R_i^2 \left(\frac{1}{R_{(k)}^2} - \frac{1}{b(n/k)^2} \right) I_{R_i \geq b(n/k)} \right| \\
&\leq \left| \frac{b(n/k)^2}{R_{(k)}^2} - 1 \right| \frac{1}{k} \sum_{i=1}^n \left| \left\langle \frac{X_i}{R_i}, \frac{Y_i}{R_i} \right\rangle \right| \left(\frac{R_i}{b(n/k)}\right)^2 I_{R_i \geq b(n/k)} \\
&\leq \left| \frac{b(n/k)^2}{R_{(k)}^2} - 1 \right| \frac{1}{k} \sum_{i=1}^n \left(\frac{R_i}{b(n/k)}\right)^2 I_{R_i \geq b(n/k)}.
\end{aligned}$$

By Lemma A.4, we have that $\frac{1}{k} \sum_{i=1}^n (R_i/b(n/k))^2 I_{R_i \geq b(n/k)} = O_P(1)$, and by Lemma A.2 (iii), we have that $b(n/k)/R_{(k)} \xrightarrow{P} 1$. Thus, $P_2(n) \xrightarrow{P} 0$. ■

Proof of Theorem 4.1. It follows from Propositions B.1 and B.2.

C Proof of Lemma 5.1 in Section 5

We begin by noting that since Z_1 and Z_2 are independent, there exists ν in $M_+(\mathbb{R}_+^2)$ such that

$$(C.1) \quad nP \left(\frac{(|Z_1|, |Z_2|)}{b(n)} \in \cdot \right) \xrightarrow{v} \nu,$$

and for $\mathbf{x} = [x_1, x_2]^\top$

$$\nu([0, \mathbf{x}]^c) = c\{(x_1)^{-\alpha} + (x_2)^{-\alpha}\}.$$

With the choice of $b(n)$ defined by

$$(C.2) \quad \begin{aligned} n^{-1} &= P(\|Z_1\phi_1\| \vee \|\rho Z_1\phi_1 + \sqrt{1-\rho^2}Z_2\phi_2\| > b(n)) \\ &= P(|Z_1| \vee (\rho^2 Z_1^2 + (1-\rho^2)Z_2^2)^{1/2} > b(n)), \end{aligned}$$

we set $c = 1/(1 + (1 - \rho^2)^{\alpha/2})$ to ensure that ν is a probability measure on $\{(z_1, z_2) : |z_1| \vee (\rho^2 z_1^2 + (1 - \rho^2)z_2^2)^{1/2} > 1\}$.

We claim that

$$(C.3) \quad \sigma_{XY} = \rho \frac{c\alpha}{\alpha - 2};$$

$$(C.4) \quad \sigma_X^2 = \frac{c\alpha}{\alpha - 2};$$

$$(C.5) \quad \sigma_Y^2 = \{\rho^2 + (1 - \rho^2)^{\alpha/2}\} \frac{c\alpha}{\alpha - 2}.$$

We first work on (C.3). Since the terms with the N_j do not affect the extremal behavior of X and Y , we have that by Proposition 4.1

$$\begin{aligned} \sigma_{XY} &= \lim_{n \rightarrow \infty} E \left[\left\langle \frac{Z_1\phi_1}{b(n)}, \frac{\rho Z_1\phi_1 + \sqrt{1-\rho^2}Z_2\phi_2}{b(n)} \right\rangle \middle| \|Z_1\phi_1\| \vee \|\rho Z_1\phi_1 + \sqrt{1-\rho^2}Z_2\phi_2\| > b(n) \right] \\ &= \lim_{n \rightarrow \infty} \frac{1}{P(\|Z_1\phi_1\| \vee \|\rho Z_1\phi_1 + \sqrt{1-\rho^2}Z_2\phi_2\| > b(n))} \times \\ &\quad E \left[\left\langle \frac{Z_1\phi_1}{b(n)}, \frac{\rho Z_1\phi_1 + \sqrt{1-\rho^2}Z_2\phi_2}{b(n)} \right\rangle I_{\|Z_1\phi_1\| \vee \|\rho Z_1\phi_1 + \sqrt{1-\rho^2}Z_2\phi_2\| > b(n)} \right] \\ &= \lim_{n \rightarrow \infty} \frac{1}{P(\|Z_1\phi_1\| \vee \|\rho Z_1\phi_1 + \sqrt{1-\rho^2}Z_2\phi_2\| > b(n))} E \left[\rho \frac{Z_1^2}{b(n)^2} I_{|Z_1| \vee (\rho^2 Z_1^2 + (1-\rho^2)Z_2^2)^{1/2} > b(n)} \right] \end{aligned}$$

It then follows from (C.1) and (C.2) that

$$\begin{aligned} \sigma_{XY} &= \lim_{n \rightarrow \infty} n E \left[\rho \frac{Z_1^2}{b(n)^2} I_{|Z_1| \vee (\rho^2 Z_1^2 + (1-\rho^2)Z_2^2)^{1/2} > b(n)} \right] \\ &= \lim_{n \rightarrow \infty} \int_{\mathbb{R}_+^2} \rho z_1^2 I_{|z_1| \vee (\rho^2 z_1^2 + (1-\rho^2)z_2^2)^{1/2} > 1} n P \left(\frac{|Z_1|}{b(n)} \in dz_1, \frac{|Z_2|}{b(n)} \in dz_2 \right) \\ &= \int_{\mathbb{R}_+^2} \rho z_1^2 I_{|z_1| \vee (\rho^2 z_1^2 + (1-\rho^2)z_2^2)^{1/2} > 1} \nu(dz_1, dz_2) \\ &= \int_{\mathbb{R}_+} \rho z_1^2 I_{\{(z_1, 0): z_1 > 1\}} c\nu_\alpha(dz_1) + \int_{\mathbb{R}_+} \rho z_1^2 I_{\{(0, z_2): z_2 > 1/(1-\rho^2)^{1/2}\}} c\nu_\alpha(dz_2) \\ &= \int_1^\infty \rho z_1^2 c\nu_\alpha(dz_1) + 0 = \rho \frac{c\alpha}{\alpha - 2}. \end{aligned}$$

Analogously, for (C.4) we can show that

$$\begin{aligned}
& \sigma_X^2 \\
&= \lim_{n \rightarrow \infty} E \left[\left\langle \frac{Z_1 \phi_1}{b(n)}, \frac{Z_1 \phi_1}{b(n)} \right\rangle \left| \left\| Z_1 \phi_1 \right\| \vee \left\| \rho Z_1 \phi_1 + \sqrt{1 - \rho^2} Z_2 \phi_2 \right\| > b(n) \right] \\
&= \lim_{n \rightarrow \infty} \frac{1}{P(\left\| Z_1 \phi_1 \right\| \vee \left\| \rho Z_1 \phi_1 + \sqrt{1 - \rho^2} Z_2 \phi_2 \right\| > b(n))} E \left[\frac{Z_1^2}{b(n)^2} I_{|Z_1| \vee (\rho^2 Z_1^2 + (1 - \rho^2) Z_2^2)^{1/2} > b(n)} \right] \\
&= \lim_{n \rightarrow \infty} n E \left[\frac{Z_1^2}{b(n)^2} I_{|Z_1| \vee (\rho^2 Z_1^2 + (1 - \rho^2) Z_2^2)^{1/2} > b(n)} \right] \\
&= \frac{c\alpha}{\alpha - 2}.
\end{aligned}$$

Next, we work on (C.5). Observe that

$$\begin{aligned}
& \sigma_Y^2 \\
&= \lim_{n \rightarrow \infty} E \left[\frac{\left\| \rho Z_1 \phi_1 + \sqrt{1 - \rho^2} Z_2 \phi_2 \right\|^2}{b(n)^2} \left| \left\| Z_1 \phi_1 \right\| \vee \left\| \rho Z_1 \phi_1 + \sqrt{1 - \rho^2} Z_2 \phi_2 \right\| > b(n) \right] \\
&= \lim_{n \rightarrow \infty} \frac{1}{P(\left\| Z_1 \phi_1 \right\| \vee \left\| \rho Z_1 \phi_1 + \sqrt{1 - \rho^2} Z_2 \phi_2 \right\| > b(n))} \times \\
&\quad E \left[\frac{\rho^2 Z_1^2 + (1 - \rho^2) Z_2^2}{b(n)^2} I_{|Z_1| \vee (\rho^2 Z_1^2 + (1 - \rho^2) Z_2^2)^{1/2} > b(n)} \right].
\end{aligned}$$

Then, again it follows from (C.1) and (C.2) that

$$\begin{aligned}
\sigma_Y^2 &= \lim_{n \rightarrow \infty} n E \left[\frac{\rho^2 Z_1^2 + (1 - \rho^2) Z_2^2}{b(n)^2} I_{|Z_1| \vee (\rho^2 Z_1^2 + (1 - \rho^2) Z_2^2)^{1/2} > b(n)} \right] \\
&= \lim_{n \rightarrow \infty} \int_{\mathbb{R}_+^2} \{ \rho^2 z_1^2 + (1 - \rho^2) z_2^2 \} I_{|z_1| \vee (\rho^2 z_1^2 + (1 - \rho^2) z_2^2)^{1/2} > 1} n P \left(\frac{|Z_1|}{b(n)} \in dz_1, \frac{|Z_2|}{b(n)} \in dz_2 \right) \\
&= \int_{\mathbb{R}_+^2} \{ \rho^2 z_1^2 + (1 - \rho^2) z_2^2 \} I_{|z_1| \vee (\rho^2 z_1^2 + (1 - \rho^2) z_2^2)^{1/2} > 1} \nu(dz_1, dz_2) \\
&= \int_{\mathbb{R}_+} \rho^2 z_1^2 I_{\{(z_1, 0): z_1 > 1\}} c\nu_\alpha(dz_1) + \int_{\mathbb{R}_+} (1 - \rho^2) z_2^2 I_{\{(0, z_2): z_2 > 1/(1 - \rho^2)^{1/2}\}} c\nu_\alpha(dz_2) \\
&= \int_1^\infty \rho^2 z_1^2 c\nu_\alpha(dz_1) + \int_{1/(1 - \rho^2)^{1/2}}^\infty (1 - \rho^2) z_2^2 c\nu_\alpha(dz_1) \\
&= \{ \rho^2 + (1 - \rho^2)^{\alpha/2} \} \frac{c\alpha}{\alpha - 2}.
\end{aligned}$$

D Consistency of $\hat{\rho}_{n,k}$ for $\alpha \in \{3, 4, 5\}$

Table 6: Empirical biases (standard errors) of $\hat{\rho}_{n,k}$ when $\alpha = 3$. The KS method is used to choose optimal k s. On average, it selects $k = 8 \sim 9$ ($N = 100$) and $k = 29 \sim 33$ ($N = 500$).

ρ_{XY}	$N = 100$	$N = 500$	ρ_{XY}	$N = 100$	$N = 500$
0	-0.002 (0.117)	0.002 (0.062)			
0.1	-0.011 (0.133)	0.000 (0.081)	-0.1	0.002 (0.130)	0.003 (0.076)
0.2	-0.009 (0.167)	-0.012 (0.109)	-0.2	0.014 (0.156)	0.008 (0.116)
0.3	-0.045 (0.185)	-0.020 (0.130)	-0.3	0.035 (0.187)	0.022 (0.124)
0.4	-0.061 (0.193)	-0.041 (0.134)	-0.4	0.055 (0.194)	0.036 (0.145)
0.5	-0.097 (0.202)	-0.052 (0.150)	-0.5	0.084 (0.190)	0.064 (0.149)
0.6	-0.127 (0.201)	-0.078 (0.159)	-0.6	0.126 (0.211)	0.080 (0.152)
0.7	-0.156 (0.197)	-0.106 (0.148)	-0.7	0.161 (0.196)	0.108 (0.150)
0.8	-0.183 (0.184)	-0.130 (0.135)	-0.8	0.194 (0.195)	0.118 (0.141)
0.9	-0.219 (0.165)	-0.142 (0.122)	-0.9	0.222 (0.168)	0.142 (0.121)
1.0	-0.222 (0.125)	-0.139 (0.079)	-1.0	0.230 (0.132)	0.141 (0.082)

Table 7: Empirical biases (standard errors) of $\hat{\rho}_{n,k}$ when $\alpha = 4$. The KS method is used to choose optimal ks . On average, it selects $k = 8$ ($N = 100$) and $k = 25 \sim 29$ ($N = 500$).

ρ_{XY}	$N = 100$	$N = 500$	ρ_{XY}	$N = 100$	$N = 500$
0	0.000 (0.172)	0.003 (0.094)			
0.1	-0.030 (0.167)	-0.019 (0.093)	-0.1	0.027 (0.163)	0.019 (0.097)
0.2	-0.053 (0.188)	-0.052 (0.114)	-0.2	0.064 (0.184)	0.051 (0.116)
0.3	-0.123 (0.198)	-0.085 (0.127)	-0.3	0.102 (0.180)	0.083 (0.130)
0.4	-0.157 (0.192)	-0.118 (0.137)	-0.4	0.147 (0.202)	0.121 (0.136)
0.5	-0.211 (0.206)	-0.155 (0.150)	-0.5	0.197 (0.196)	0.163 (0.140)
0.6	-0.253 (0.202)	-0.204 (0.146)	-0.6	0.256 (0.199)	0.209 (0.154)
0.7	-0.306 (0.202)	-0.249 (0.156)	-0.7	0.315 (0.205)	0.255 (0.154)
0.8	-0.366 (0.207)	-0.291 (0.150)	-0.8	0.366 (0.206)	0.291 (0.150)
0.9	-0.415 (0.193)	-0.340 (0.141)	-0.9	0.415 (0.200)	0.329 (0.142)
1.0	-0.410 (0.170)	-0.326 (0.124)	-1.0	0.428 (0.171)	0.325 (0.126)

Table 8: Empirical biases (standard errors) of $\hat{\rho}_{n,k}$ when $\alpha = 5$. The KS method is used to choose optimal ks . On average, it selects $k = 7 \sim 8$ ($N = 100$) and $k = 18 \sim 20$ ($N = 500$).

ρ_{XY}	$N = 100$	$N = 500$	ρ_{XY}	$N = 100$	$N = 500$
0	-0.007 (0.199)	-0.004 (0.159)			
0.1	-0.046 (0.208)	-0.043 (0.144)	-0.1	0.053 (0.195)	0.041 (0.145)
0.2	-0.087 (0.204)	-0.095 (0.145)	-0.2	0.097 (0.202)	0.096 (0.158)
0.3	-0.173 (0.210)	-0.147 (0.149)	-0.3	0.155 (0.201)	0.142 (0.161)
0.4	-0.229 (0.198)	-0.203 (0.151)	-0.4	0.212 (0.209)	0.196 (0.161)
0.5	-0.289 (0.202)	-0.263 (0.164)	-0.5	0.279 (0.206)	0.264 (0.156)
0.6	-0.351 (0.217)	-0.324 (0.172)	-0.6	0.356 (0.207)	0.330 (0.184)
0.7	-0.411 (0.206)	-0.388 (0.171)	-0.7	0.424 (0.210)	0.397 (0.157)
0.8	-0.491 (0.209)	-0.458 (0.170)	-0.8	0.491 (0.207)	0.446 (0.162)
0.9	-0.556 (0.207)	-0.511 (0.156)	-0.9	0.554 (0.207)	0.505 (0.163)
1.0	-0.548 (0.171)	-0.502 (0.143)	-1.0	0.564 (0.178)	0.509 (0.149)